

Review

Theory of Projectors and Its Application to Molecular Symmetry

Horace T. Crogman ^{1,2} 

¹ Physics Department, California State University Dominguez Hills, Carson, CA 90747, USA; hcrogman@csudh.edu or hcrogman@gmail.com; Tel.: +1-310-234-2092

² The Institute for Effective Thinking, Riverside, CA 92508, USA

Abstract: Projector theory can serve as a powerful tool to perform the symmetric computation of molecular systems. The work of William Harter has long demonstrated the effectiveness of this theory in molecular spectroscopy; however, it seems its usefulness has not been realized by many in the field. We have described this methodology and have considered the D_3 symmetry system and the tetrahedral symmetry of methane molecules as concrete examples where the computed rotation tensors and vibrational wavefunction were derived for some symmetry states.

Keywords: projectors; eigenvalues; eigenvectors; symmetry; all-commuting-operators; wave-function; rovibrational Hamiltonian

1. Introduction

In some sense, we have a closed-form solution of the Schrodinger equation for the hydrogen molecule, but, beyond this, there are no closed-form solutions for any other molecule. However, with the aid of numerical techniques, we can solve the molecular problem with a great degree of accuracy. As more and more larger molecules are considered, techniques tend to have limitations. Many clever approaches result in all sorts of approximation schemes, which work well for some systems but not for others. Paousek and Aliev [1] have shown that the general molecular Hamiltonian to is given by,

$$H_i = \sum_{j=1}^{N_e} \left(\frac{\hbar^2}{2m_e} p_j^2 \right) + \sum_{i=1}^N \left(\frac{\hbar^2}{2m} P_i^2 \right) - V, \quad (1)$$

where $p_i(\dot{x}_j, \dot{y}_j, \dot{z}_j)$ is the momentum of electrons and $P_i(\dot{x}_i, \dot{y}_i, \dot{z}_i)$ is the momentum of the nuclei. It does not lend itself to a description of the stationary states of a polyatomic molecule. Although the Hamiltonian is of a simple form, the numerical integration of the Hamiltonian in terms of the space-fixed coordinates of the atomic nuclei and electrons is extremely difficult, even for the simplest of molecular systems [2–4].

A classical description of such a system of atomic nuclei and electrons sometimes reveals translation and rotation motion in space. The atomic nuclei can vibrate around the configuration given by the electronic structure of the molecule, and the electron also can move around the atomic nuclei. As a result, a quantum mechanical description of these motions should yield vibrational, rotational, and electronic energy levels and the corresponding wave function of the Schrodinger equation for this system. The task, however, of getting the information from a full Schrodinger wave equation is almost impossible, therefore, other techniques must be explored [1–4].

One approach is to develop a classical model of its translation, overall rotation, the vibration of the atomic nuclei, and the electronic motions. This is achieved by replacing the laboratory or the space-fixed coordinates of the atomic nuclei and electrons with new coordinate systems suitable for describing the individual types of motion mentioned above [3,4]. The Hamiltonian is developed in the new coordinates $x_j, y_j, z_j (j = 1, 2, \dots, N_e)$, which are the coordinates of the electrons concerning a moving x, y, z axis system fixed to



Citation: Crogman, H.T. Theory of Projectors and Its Application to Molecular Symmetry. *Symmetry* **2023**, *15*, 496. <https://doi.org/10.3390/sym15020496>

Academic Editor: Evgeny Nikulchev

Received: 18 January 2023

Revised: 4 February 2023

Accepted: 7 February 2023

Published: 13 February 2023



Copyright: © 2023 by the author. Licensee MDPI, Basel, Switzerland. This article is an open access article distributed under the terms and conditions of the Creative Commons Attribution (CC BY) license (<https://creativecommons.org/licenses/by/4.0/>).

a molecule. The Euler angles θ, ϕ, χ define the orientation of the x, y, z axis system with respect to the X, Y, Z axis system. The coordinates $Q_1, Q_2, \dots, Q_{3N-6}$ are the vibrational displacement vectors of the system atomic nuclei for the x, y, z axis system [1–5]. Next, we make the Born–Oppenheimer approximation (BOA) to obtain a Hamiltonian for the electronic state and a Hamiltonian for vibrational–rotational states for given electronic states. Furthermore, Born–Oppenheimer-like approximations allow for the separation of the vibrational motions from the rotational motion [1–8].

The BOA allows the molecular Hamiltonian to be separated into the electronic part and its rovibrational Hamiltonian. The rovibrational Hamiltonian is given by

$$H_{rv} = \underbrace{AJ_x^2 + BJ_y^2 + CJ_z^2}_{H_r^0} + \underbrace{\sum_k P_k^2 + \frac{1}{2} \sum_{k=1}^{2N-6} \lambda_k Q_k^2}_{H_v^0} + V, \quad (2)$$

where

$$A = \frac{1}{2I_x}, B = \frac{1}{2I_y}, C = \frac{1}{2I_z}, \quad (3)$$

and H_r^0 is the rotational Hamiltonian, and H_v^0 is a harmonic oscillator Hamiltonian. The wavefunction for the molecule is given by,

$$\Psi = \psi_e(r_{j\alpha}^0) \psi_e^0(Q_1, Q_2, \dots) \psi_r^0(\phi, \theta, \chi). \quad (4)$$

Here, we can exploit the spatial symmetry of the molecule in the molecular system. A symmetry operation is a geometrical action that leaves the position of the atoms unchanged. There are five types of geometry operations: Identity (1), reflection (σ), rotation (C_n), rotation–reflection (S_n), and inversion (i). Each symmetry operation, excluding the identity, is associated with a symmetry element [1–4,8,9]. The symmetry operation is the actual action, while the symmetry element is the point, line, or plane about which the action occurs. Therefore, our goal in this paper is to illustrate how symmetry analysis can calculate genuine vibrations and classify the spectra according to the point group irreps. Thus, spectral decomposition is a powerful tool that will aid in determining the eigenvectors and the eigenvalues if the symmetry group is known. Harter [3,8] has detailed descriptions of the procedure for such a computation. We will outline how to utilize this method to perform calculations on a tetrahedral molecule. The key in this approach is to determine the projectors associated with the particular group symmetries.

2. Commuting Observable and Symmetry Projectors

Symmetry groups are classified into two categories: Abelian and Non-Abelian. The neat thing about Abelian groups is that we can write all the class operators as a combination of a single set of idempotent projectors. However, this is not the case for Non-Abelian groups. For the very simple fact that every group operator does not commute. All is not lost because we can find a set of mutually commuting operators. We describe how to do this by following the procedure outlined by Harter [3,8]. Moreover, similar approaches have been described in [4,7,9–18].

- A. **Class algebra and all-commuting operator.** We create the class structure of the group. This allows us to create communicative algebra. Each class sum commutes with each other and with every operator in the entire group algebra. In other words, the cg 's are mutually commuting with respect to themselves and all-commuting with respect to the whole group. $\sum_{g=1}^{\circ G} hgh^{-1} = n_g c_g$. Harter [3,8] showed that an all-commuting operator $C = C_g g$ that is, one that commutes with all h in the group, is a combination of class sums cg . All commutation ($C h = h C$) implies,

$$C = \sum_{g=1}^{\circ G} c_g g = \frac{1}{\circ G} \sum_{h=1}^{\circ G} h \left(\sum_{g=1}^{\circ G} c_g g \right) h^{-1} = \sum_{g=1}^{\circ G} c_g n_g c_g \tag{5}$$

B. Characters and all-commuting projectors. We construct the projectors by solving the minimal equation of the group,

$$\mathbb{P}^\alpha = \frac{\prod_{\gamma \neq \alpha} (c_i - c_s^\gamma 1)}{\prod_{\gamma \neq \alpha} (c_s^\alpha - c_s^\gamma)} \tag{6}$$

where \mathbb{P}^α are called the All-Commuting Class Idempotent (ACCI), and c_s^α and c_s^γ are eigenvalues from the minimal equation. We can expand the original class operators in terms of all commuting idempotent [3] i.e.,

$$c_j = \sum_{\alpha} c_j^\alpha \mathbb{P}^\alpha \tag{7}$$

where c_j^α is the eigenvalue such that $c_j \mathbb{P}^\alpha = c_j^\alpha \mathbb{P}^\alpha$. By knowing the character table of the group, (5) can be obtained from,

$$P^\alpha = \sum_{m=1}^{\ell^\alpha} P_m^\alpha = \frac{\ell^\alpha}{\circ G} = \sum_{m=1}^{\ell^\alpha} D_{mm}^\alpha(g) g = \frac{\ell^\alpha}{\circ G} \sum_{m=1}^{\ell^\alpha} \chi^\alpha(g) g \tag{8}$$

Next, we acquire the inverse of (7), which must satisfy the completeness and spectral decomposition relation, i.e.,

$$1 = \sum_{\alpha} \mathbb{P}^\alpha \text{ and } g = \sum_{k=0}^{n-1} D^{k_n}(g) \mathbb{P}^{k_n} \tag{9}$$

The way we performed the spectral decomposition will depend on whether the group is Abelian or Non-Abelian. For Abelian grouping, an element g must satisfy a minimal equation $g^n = 1$ where there exists n orthogonal idempotents $\{p^1, p^2, \dots, p^n\}$. We must choose another element h of the group that would yield $\{q^1, q^2, \dots, q^n\}$. Both sets must satisfy the completeness and the spectral decomposition equation,

$$\sum_{j=1}^n p^j = 1 = \sum_{j=1}^m q^j \tag{10}$$

We then multiply (9) by p^j , which may result in the splitting of p^j into a sum of operators $p^j q^k$,

$$p^j = p^1 q^1 + p^2 q^2 + \dots + p^j q^k = \dots + \mathbb{P}^2 + \mathbb{P}^2 + \dots + \mathbb{P}^r \quad r \leq m. \tag{11}$$

This set of nonzero terms $\{\mathbb{P}^1, \mathbb{P}^2, \dots, \mathbb{P}^n\}$ will also satisfy orthonormality and completeness relations. Therefore, the spectral decomposition of g and h ,

$$g = \sum_{j=1} D^j(g) \mathbb{P}^j \text{ and } h = \sum_{j=1} D^j(h) \mathbb{P}^j \tag{12}$$

C. Maximal sets of commuting operators (MSOCO). These are the independent operators of the group that can be diagonalized at once. They are not unique since there are numerous sets of operators that compete to be part of a specialized set called an MSOCO (Maximal Set of Commuting Operators or Observables (MSOCO) [3,8]. The number of operators is the rank of the group. As an example, shown in [8], the rank of D_3 turns out to be four. Furthermore, the set diagram of D_3 in Figure 1 shows the class sum algebra of all-commuting operators at the center of the diagram.

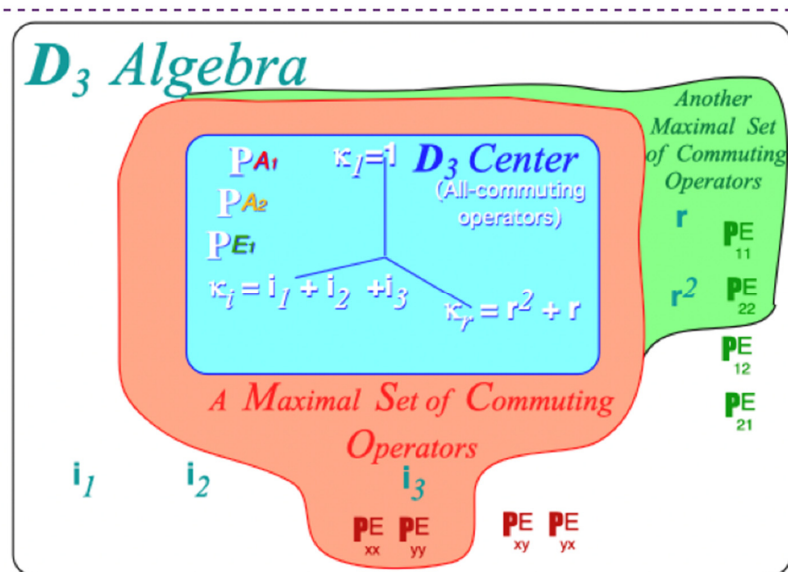


Figure 1. D_3 Algebra and sub-algebras [8]. This describes the Maximal Set of Commuting Operators (MSOCO). The operators in the blue shaded region at the center are referred to as all-commuting operators. The other operators in the other shaded regions are temporarily remaining non-unique members of MSOCO. When choosing an operator in one of these other regions, we split P^E idempotent in a particular manner.

The D_3 dimension determines the number of orthogonal irreducible representations (irreps) in the algebra (the irreps A_1 , A_2 , and E and the three all-commuting projectors $\{P^{A_1}, P^{A_2}, P^E\}$ of the center are uniquely defined; no others exist). A rank of four implies another member of the MSOCO. The rank can be obtained by simply summing down the column of the character table (13). From the first column of the character table, we are able to tell how each irrep will split.

D_3	1	r, r^2	i_1, i_2, i_3	
A_1	1	1	1	
A_2	1	1	-1	
E	2	-1	0	(13)

The other member of the rank-4 MSOCO is not uniquely chosen; one choice is the operator i_3 picked in Figure 1 (other choices are shown in the figure). By choosing this operator to be diagonal, we are selecting a particular way to “split” the P^E idempotent and build a particular set of E -irreps. Furthermore, the number of operators needed depends on the order of group. Thus, in the case of D_3 there are six projectors needed. In general, the number of operators needed is given by,

$$\circ G = \sum_{\alpha} (\ell^{\alpha})^2 \tag{14}$$

In the case of tetrahedral symmetry, the rank is 10 but only 5 irreps are possible: A_1 , A_2 , E , T_1 , and T_2 and total number operators is 24. However, T_1 is not vibrational mode and, thus, only 15 operators are necessary.

D. Computing irreducible projectors. To compute the irreducible projectors of a non-communicating group we must consider the projectors of its subgroups. The key is finding the non-commutative spectral decomposition of the entire Non-Abelian group. Unlike Abelian, Non-Abelian will consist of nilpotent ($\mathbb{P}^2 = 0$) and idempotent ($\mathbb{P}^2 = \mathbb{P}$) projectors. Nilpotent projectors are important for expanding operators that do not commute. Each of the all-commuting idempotents \mathbb{P}^{α} can be split into ℓ^{α} irreducible idempotents, i.e.,

$$\mathbb{P}^\alpha = P_1^\alpha + P_2^\alpha + \dots + P_{\ell^\alpha}^\alpha \tag{15}$$

If $\ell^\alpha = 1$, then \mathbb{P}^α remains un-split. We use the subgroup idempotent to split \mathbb{P}^α . Suppose that $H \subseteq G$ where μ and α are the irreps of H and G , respectively, such that $\{P_1^\mu, P_2^\mu, \dots, P_{\ell^\mu}^\mu\}$ are projectors of H and $\{\mathbb{P}^{\alpha_1}, \mathbb{P}^{\alpha_2}, \dots, \mathbb{P}^{\alpha_n}\}$ are projectors of G , then idempotent of both H and G satisfy the completeness relation,

$$1 = \sum_{k=1}^{\ell^\alpha} P_k^\mu \text{ and } 1 = \sum_{k=1}^n P_k^\alpha, \tag{16}$$

such that:

$$1 \cdot 1 = \left(\sum_{k=1}^{\ell^\alpha} P_k^\mu \right) \left(\sum_{k=1}^n P_k^\alpha \right) = \sum_{k=1}^n P_i^{\alpha_i} \tag{17}$$

Hater [3] refers to this as one times one ($1 \cdot 1$) trick. Thus, a single projector such that $\ell^\alpha > 1$ will split as,

$$\mathbb{P}^{\alpha_1} = \mathbb{P}^{\alpha_1} 1 = \mathbb{P}^{\alpha_1} \sum_{k=1}^{\ell^\mu} P_k^\mu = P_1^{\alpha_1} + P_2^{\alpha_1} + \dots + P_r^{\alpha_1} \tag{18}$$

Every subgroup will give a different splitting. For octahedral [3], the all-commuting idempotent \mathbb{P}^{T_1} splits when multiplied by six idempotents of D_4 :

$$\mathbb{P}^{T_1} = \mathbb{P}^{T_1} 1 = \mathbb{P}^{T_1} (P_1^E + P_2^E + P^{A_1} + P^{A_2} + P^{B_1} + P^{B_2}) = P_1^{T_1} + P_2^{T_1} + 0 + P_3^{T_1} + 0 + 0 \tag{19}$$

Let's consider D_3 symmetry a much simpler group with rank 4 and three irreps see (13). Of the three irreps only $\mathbf{P}^3 = \mathbf{P}^E$ splits. Since C_2 is a subgroup of D_3 we use it to decompose \mathbf{P}^E into the irreducible projectors P_{xx}^E and P_{yy}^E shown below,

$$\begin{aligned} \mathbf{P}^E \mathbf{P}^x &= \mathbf{P}^x \mathbf{P}^E = (1 + \mathbf{i}_3)/2 (21 - \mathbf{r} - \mathbf{r}^2)/3 = (21 - \mathbf{r} - \mathbf{r}^2 - \mathbf{i}_1 - \mathbf{i}_2 + 2\mathbf{i}_3)/6 = \mathbf{P}_{xx}^E, \\ \mathbf{P}^E \mathbf{P}^y &= \mathbf{P}^y \mathbf{P}^E = (1 - \mathbf{i}_3)/2 (21 - \mathbf{r} - \mathbf{r}^2)/3 = (21 - \mathbf{r} - \mathbf{r}^2 + \mathbf{i}_1 + \mathbf{i}_2 - 2\mathbf{i}_3)/6 = \mathbf{P}_{yy}^E. \end{aligned} \tag{20}$$

Now using the ($1 \cdot 1$) trick with the completeness relation gives,

$$\mathbf{1} = \mathbf{1} \cdot \mathbf{1} = (\mathbf{P}^{A_1} + \mathbf{P}^{A_2} + \mathbf{P}^E)(\mathbf{P}^x + \mathbf{P}^y) = \mathbf{P}^{A_1} + \mathbf{P}^E + \mathbf{P}_{xx}^E + \mathbf{P}_{yy}^E \tag{21}$$

Next, $\mathbf{1}$ is wrapped around any operator \mathbf{g} of the D_3 algebra to give the following generalized **Spectral Decomposition** of the form shown in (22),

$$\mathbf{g} = \mathbf{1} \mathbf{g} \mathbf{1} = (\mathbf{P}^{A_1} + \mathbf{P}^{A_2} + \mathbf{P}_{xx}^E + \mathbf{P}_{yy}^E) \cdot \mathbf{g} \cdot (\mathbf{P}^{A_1} + \mathbf{P}^{A_2} + \mathbf{P}_{xx}^E + \mathbf{P}_{yy}^E). \tag{22}$$

Thus, this result in (21) in which the \mathbf{P}^{A_1} and \mathbf{P}^{A_2} are unchanged because they are all-commuting,

$$\mathbf{g} = \mathbf{1} \mathbf{g} \mathbf{1} = \mathbf{g} \mathbf{P}^{A_1} + \mathbf{g} \mathbf{P}^{A_2} + \mathbf{P}_{xx}^E \cdot \mathbf{g} \mathbf{P}_{xx}^E + \mathbf{P}_{xx}^E \cdot \mathbf{g} \mathbf{P}_{yy}^E + \mathbf{P}_{yy}^E \cdot \mathbf{g} \mathbf{P}_{xx}^E + \mathbf{P}_{yy}^E \cdot \mathbf{g} \mathbf{P}_{yy}^E \tag{23}$$

The remaining four terms are the E -projectors multiplied by irreps as seen by comparing (24)

$$\begin{aligned} \mathbf{P}_{xx}^E \cdot \mathbf{g} \mathbf{P}_{xx}^E &= D_{xx}^E(\mathbf{g}) \mathbf{P}_{xx}^E, \quad \mathbf{P}_{xx}^E \cdot \mathbf{g} \mathbf{P}_{yy}^E = D_{xy}^E(\mathbf{g}) \mathbf{P}_{xy}^E, \\ \mathbf{P}_{yy}^E \cdot \mathbf{g} \mathbf{P}_{xx}^E &= D_{yx}^E(\mathbf{g}) \mathbf{P}_{yx}^E, \quad \mathbf{P}_{yy}^E \cdot \mathbf{g} \mathbf{P}_{yy}^E = D_{yy}^E(\mathbf{g}) \mathbf{P}_{yy}^E. \end{aligned} \tag{24}$$

(23) is the form of a generalized non-commutative spectral decomposition of an entire Non-Abelian group. D_3 's decomposition differs from the commutative C_6 . D_3 has two

nilpotent projectors \mathbf{P}_{xy}^E and \mathbf{P}_{yx}^E along with four ordinary (idempotent) projectors \mathbf{P}^{A_1} , \mathbf{P}^{A_2} , \mathbf{P}_{xx}^E , and \mathbf{P}_{yy}^E . Other Non-Abelian groups have other numbers of these two kinds of \mathbf{P} 's.

All commutative groups can be reduced to orthogonal idempotents that satisfy simple orthogonality relations given in [4],

$$\mathbf{P}_i \mathbf{P}_j = \delta_{ij} \mathbf{P}_i = \mathbf{P}_j \mathbf{P}_i. \tag{25}$$

A more general formulation spectral decomposition comes from writing (12) as,

$$g = 1g1 = \left(\sum_{k=1}^{\ell^\alpha} P_k^\mu \right) g \left(\sum_{k=1}^n P_k^\alpha \right) = \sum_{\mu} \sum_m \sum_n D_{mn}^\mu(g) P_{mn}^\mu \tag{26}$$

and (25) replaced by the generalized projector orthonormality relation for non-commutative projectors,

$$P_{jk}^\mu P_{mn}^\nu = \delta^{\mu\nu} \delta_{mn} P_{jn}^\mu \tag{27}$$

To obtain generalized projectors, the decomposition (26) must be inverted. The result which will be proved below is the famous Wigner–Weyl projection formula,

$$P_{mn}^\mu = \frac{\ell^\mu}{\circ G} \sum_g D_{mn}^{\mu*}(g) g. \tag{28}$$

where $\circ G = 6$ is the order of the group D_3 and ℓ^m is the m-irrep dimension, ($\ell^{A_1} = 1$, $\ell^{A_2} = 1$, and $\ell^{E_1} = 2$). Again, these numbers vary from group to group. For Abelian groups, irrep dimensions are always one ($\ell^m = 1$).

Let us summarize the first set of six irrep projectors which will be used in a band theory model below,

	P^{A_1}	P^{A_2}	$P_{xx}^E = P_x^E 1 P_x^E$	$P_{yy}^E = P_y^E 1 P_y^E$	$P_{xy}^E = D_{xy}^E(i_3) P^E = P_x^E i_3 P_y^E$	$P_{yx}^E = D_{yx}^E(i_3) P_{yx}^E = P_y^E i_3 P_x^E$
1	1	1	2	2	0	0
r	1	1	-1	-1	-1	1
r^2	1	1	-1	-1	1	-1
i_1	1	-1	-1	1	-1	-1
i_2	1	-1	-1	1	1	1
i_3	1	-1	2	-2	0	0
	1/6	1/6	1/6	1/6	1/4	1/4

(29)

The element i_2 is outside of the CSOCO can be used to determine the two non-zero nilpotent projectors \mathbf{P}_{xy}^E and \mathbf{P}_{yx}^E since the idempotents \mathbf{P}_{xx}^E and \mathbf{P}_{yy}^E from (29) are orthogonal. A commuting operator would permit the two projectors to annihilate [8]. The key is to choose any operator such as r , r^2 , i_1 , or i_2 outside of the CSOCO, as shown in Figure 1. This will give all the needed projectors. At this stage, we use the projector to find eigenvalues and eigenvectors,

$$|e_{jk}^\alpha A\rangle = \frac{P_{jk}^\alpha |A\rangle}{\sqrt{N_k^\alpha}} \tag{30}$$

Suppose that we have the normalized eigenfunction $|e_j^\alpha\rangle = P_{jk}^\alpha |1\rangle / \sqrt{N_k^\alpha}$, then the vector product is $\langle e_j^\alpha | e_j^\alpha \rangle = 1$ gives,

$$N_k^\alpha = \langle 1 | P_{jk}^\alpha P_{jk}^\alpha | 1 \rangle = \langle 1 | P_{kk}^\alpha | 1 \rangle \tag{31}$$

Given this and the irrep **P**-operators in (29), the D_3 -symmetry projected states are obtained easily,

	$ P^{A_1}\rangle$	$ P^{A_2}\rangle$	$ P_{xx}^E\rangle$	$ P_{yy}^E\rangle$	$ P_{xy}^E\rangle$	$ P_{yx}^E\rangle$
1	1	1	2	2	0	0
r	1	1	-1	-1	-1	1
r^2	1	1	-1	-1	1	-1
i_1	1	-1	-1	1	-1	-1
i_2	1	-1	-1	1	1	1
i_3	1	-1	2	-2	0	0
	$1/\sqrt{6}$	$1/\sqrt{6}$	$1/2\sqrt{3}$	$1/2\sqrt{3}$	$1/2$	$1/2$

(32)

The E-matrices $D^E(\mathbf{g}) = \begin{pmatrix} D_{11}^E & D_{12}^E \\ D_{21}^E & D_{22}^E \end{pmatrix}$ we can derive from the projector states for example $D^E(r) = \begin{pmatrix} \frac{1}{2} & \frac{\sqrt{3}}{2} \\ \frac{\sqrt{3}}{2} & \frac{1}{2} \end{pmatrix}$; This comes about by computing the operator r acts on the column element $|P_{11}^E\rangle$ and $|P_{21}^E\rangle$ (i.e., $r|P_{11}^E\rangle$ and $r|P_{21}^E\rangle$),

$$r|P_{11}^E\rangle = r(2 - r - r^2 - i_1 - i_2 + 2i_3) / 2\sqrt{3} = \begin{pmatrix} -1 \\ 2 \\ -1 \\ -1 \\ -1 \end{pmatrix} / 2\sqrt{3}$$

$$= \frac{-\frac{1}{2}|P_{11}^E\rangle + \frac{\sqrt{3}}{2}|P_{21}^E\rangle}{2\sqrt{3}},$$
(33)

$$r|P_{21}^E\rangle = r(0 + r - r^2 - i_1 + i_2 + 0i_3) / 2\sqrt{3} = \begin{pmatrix} 1 \\ 0 \\ -1 \\ 1 \\ 0 \\ 1 \end{pmatrix} / 2\sqrt{3}$$

$$= \frac{-\frac{\sqrt{3}}{2}|P_{11}^E\rangle + \frac{1}{2}|P_{21}^E\rangle}{2\sqrt{3}}.$$
(34)

We compute the following products, $D_{11}^E = \langle P_{11}^E | r | P_{11}^E \rangle$, $D_{21}^E = \langle P_{21}^E | r | P_{11}^E \rangle$, $D_{12}^E = \langle P_{12}^E | r | P_{21}^E \rangle$, and $D_{22}^E = \langle P_{12}^E | r | P_{21}^E \rangle$. In general,

$$\langle P_{ij}^\alpha | \mathbf{g} | P_{kl}^\beta \rangle = D_{ik}^\alpha(\mathbf{g}) \delta^{\alpha\beta} \delta_{jl},$$
(35)

and

$$\mathbf{g} | P_{ij}^\alpha \rangle = \sum_{k=1}^l D_{ki}^\alpha(\mathbf{g}) | P_{kj}^\alpha \rangle$$
(36)

Thus, from (33)–(36) we found all reduce regular representation for our D_3 example as shown by (37),

$\mathbf{g} =$	1	r	r^2	i_1	i_2	i_3
$D^{A_1}(\mathbf{g}) =$	1	1	1	1	1	1
$D^{A_2}(\mathbf{g}) =$	1	1	1	-1	-1	-1
$D_{x_2 y_2}^E(\mathbf{g}) =$	$\begin{pmatrix} 1 & . \\ . & 1 \end{pmatrix}$	$\begin{pmatrix} -1/2 & -\sqrt{3}/2 \\ \sqrt{3}/2 & -1/2 \end{pmatrix}$	$\begin{pmatrix} -1/2 & \sqrt{3}/2 \\ -\sqrt{3}/2 & -1/2 \end{pmatrix}$	$\begin{pmatrix} -1/2 & -\sqrt{3}/2 \\ -\sqrt{3}/2 & 1/2 \end{pmatrix}$	$\begin{pmatrix} -1/2 & \sqrt{3}/2 \\ \sqrt{3}/2 & 1/2 \end{pmatrix}$	$\begin{pmatrix} 1 & . \\ . & -1 \end{pmatrix}$

(37)

Each bra or ket is an operation of **P**-operator on the “first” state $|1\rangle$. Note the use of conjugation: $P_{m n}^\dagger = P_{n m}$.

3. Rovibrational Hamiltonian and Wavefunctions

In (2), we write down the rovibrational Hamiltonian for a molecular system. This is synonymous with that described by Bunker and Jensen [4]. Bunker and Jensen [4] showed that invoking the harmonic oscillator approximation leads to the rigid-rotor harmonic oscillator Hamiltonian for a rotational–vibrational motion. Consequently, our Hamiltonian is given by,

$$H = \frac{1}{2} \sum_{\alpha} \mu_{\alpha\alpha}^e J_{\alpha}^2 + \sum_{\alpha} \sum_i \left[\frac{(p_2^{\alpha})^2}{2} + \frac{(\omega^{\alpha} q_2^{\alpha})^2}{2} \right], \tag{38}$$

where

$$\frac{\partial H}{\partial p_i^{\alpha}} = \dot{q}_i^{\alpha} = p_i^{\alpha} \tag{39}$$

This is then treated as a quantum oscillator, as em-modes are quantized to give quantum field theory. The quantum theory of vibrational modes has the same traditional classical roots as quantum field theory. We will use canonical variables, which are defined by

$$q_j^{\alpha} = \langle e_j^{\alpha} | m | x \rangle, \quad p_j^{\alpha} = \langle e_j^{\alpha} | m | \dot{x} \rangle \tag{40}$$

Next, we write the canonical variables in ordinary coordinates.

$$X_{IQ} = \langle IQ | x \rangle. \tag{41}$$

Using the completeness relation gives

$$\begin{aligned} X_{IQ} = \langle IQ | x \rangle &= \sum_{\alpha} \sum_j \langle IQ | e_j^{\alpha} \rangle \langle e_j^{\alpha} | m | x \rangle \\ &= \sum_{\alpha} \sum_l \langle IQ | e_j^{\alpha} \rangle q_j^{\alpha} \end{aligned} \tag{42}$$

where

$$q_j^{\alpha} = \sum_{Q=A_1, E, T_2} \sum_l \langle e_j^{\alpha} | m | IQ \rangle \langle IQ | x \rangle. \tag{43}$$

We can then write annihilation and creation operators in terms of symmetry coordinates since

$$a_i^{\alpha} = \left[\sqrt{\omega^{\alpha}} q_i^{\alpha} + \frac{i}{\sqrt{\omega^{\alpha}}} p_i^{\alpha} \right] / \sqrt{2\hbar}, \tag{44}$$

$$a_i^{\alpha\dagger} = \left[\sqrt{\omega^{\alpha}} q_i^{\alpha} - \frac{i}{\sqrt{\omega^{\alpha}}} p_i^{\alpha} \right] / \sqrt{2\hbar}. \tag{45}$$

We can consider how to symmetrize the wavefunction for the rovibrational Hamiltonian. Dijon group [19,20] define a compact form that can be expressed as,

$$|\Psi_{rv}^{\Gamma, \gamma}\rangle = \left[|\Psi_{rot}^{\Gamma_1}\rangle \times |\Psi_{vib}^{\Gamma_2}\rangle \right]_{\gamma}^{\Gamma}. \tag{46}$$

We consider the form for the vibration and rotation as describe by ref. [9,10],

$$|\Psi_{rot}^{\Gamma_1}\rangle = \sum_{k=-J}^J s_{k; \Gamma, \gamma}^J |Jkm\rangle \tag{47}$$

$$|Jkm\rangle = D_{mk}^J(\alpha\beta\gamma) / \sqrt{\frac{8\pi^2}{2j+1}} \tag{48}$$

where

$$D_{mk}^J(g) = \frac{\sqrt{(J-m)!(J+m)!} \sqrt{(J-k)!(J+k)!} \times \sum_n (-1)^n \left(\cos \frac{\beta}{2}\right)^{2J+m-k-2n} \left(\sin \frac{\beta}{2}\right)^{k-m+2n} e^{-i(m\alpha+k\gamma)}}{(J+m-n)!(k-m+n)!n!(J-k-n)!} \tag{49}$$

and $s_{k;\Gamma,\gamma}^J$ or similarly in spherical harmonics by Wormer [21]

$$|l, m, G, \lambda, i\rangle = \frac{f_\lambda}{|G|} \sum_{g \in G} D^{(\lambda)}(g^{-1})_{ij} g Y_{lm} \tag{50}$$

A. Rotational Wavefunction

To $|\Psi_{rot}^{\Gamma_1}\rangle$, we must consider the overall external symmetry O_3 . This then correlated with the internal symmetry Γ_1 . Knowing Γ_1 gives a correlation induced between the irrep Γ_1 and that of O_3 . The characters of R_3 are given by,

$$Trace D^\ell(\omega 00) = \frac{\sin\left(\ell + \frac{1}{2}\right)\omega}{\sin \omega/2} \tag{51}$$

We derive the character of O_3 from its outer product in relation to R_3 in (51).

Trace $D(\omega 00) =$

O_3	1 $\omega = 0^\circ$	r, r^2 $\omega = 120^\circ$	R^2 $\omega = 180^\circ$	R, R^3 $\omega = 90^\circ$	i $\omega = 180^\circ$	I $\omega = -180^\circ$	Ir, Ir^2 $\omega = 120^\circ$	IR^2 $\omega = 180^\circ$	IR, IR^3 $\omega = 90^\circ$	Ii $\omega = 180^\circ$
0^+	1	1	1	1	1	1	1	1	1	1
0^-	1	1	1	1	1	-1	-1	-1	-1	-1
1^+	3	0	-1	1	-1	3	0	-1	1	-1
1^-	3	0	-1	1	-1	-3	0	1	-1	1
2^+	5	-1	1	-1	1	5	-1	1	-1	1
2^-	5	-1	1	-1	1	-5	1	-1	1	-1
3^+	7	1	-1	-1	-1	7	1	-1	-1	-1
3^-	7	1	-1	-1	-1	-7	-1	1	1	1
4^+	9	0	1	1	1	9	0	1	1	1
4^-	9	0	1	1	1	-9	0	-1	-1	-1
5^+	11	-1	-1	1	-1	11	-1	-1	1	-1
5^-	11	-1	-1	1	-1	-11	1	-1	1	1
6^+	13	1	1	-1	1	13	1	1	-1	1

The frequency $f^{\Gamma_1}(J)$ of the irreducible representation of Γ_1 subduced to R_3 is given by:

$$f^{\Gamma_1} = \frac{1}{|G|} \sum_{classes\ c_g} \chi_g^{\Gamma_1^*} c_g Trace D^\ell(g) \tag{53}$$

where Γ_1 is the irrep label of the point group of the composite rigid body. With $\Gamma_1 = T_d$ the Equation (53) and we can use character table (54) to find the induced representation,

T_d	1	$(r_1 \dots r_1^2 \dots)$	$(R_1^2 \dots)$	$(IR_1 \dots IR_3^3 \dots)$	$(Ii_1 \dots)$
A_1	1	1	1	1	1
A_2	1	1	1	-1	-1
E	2	-1	2	0	0
T_1	3	0	-1	1	-1
T_2	3	0	-1	-1	1

Therefore, we give the correlation between R_3 and T_d as (55),

$T_d \uparrow O_3$	A_1	A_2	E	T_1	T_2
$S_4 \uparrow O_3$	$\{4\}$	$\{1^4\}$	$\{2^2\}$	$\{2, 1^2\}$	$\{3, 1\}$
$J^p = 0^+$	1
0^-	.	1	.	.	.
1^+	.	.	.	1	.
1^-	1
2^+	.	.	1	.	1
2^-	.	.	1	1	.
3^+	.	1	.	1	1
3^-	1	.	.	1	1
4^+	1	.	1	2	1
4^-	.	1	1	1	2
5^+	.	.	1	2	1
5^-	.	.	1	1	2
6^+	1	1	1	1	2
6^-	1	1	1	2	1
7^+	1	.	1	2	2
7^-	.	1	1	2	2

We construct symmetrize rotational wave function as follows

$$|\Gamma_1 \gamma\rangle = P_{\gamma f}^{\Gamma_1} |J \rangle_{mk} / \sqrt{N^{\Gamma_1}} = \frac{1}{\sqrt{N^{\Gamma_1}}} \sum_{R_l} D_{\gamma f}^{\Gamma_1}(R_l) R_l |J \rangle_{mk} \tag{56}$$

$$R_l |J \rangle_{mk} = \sum_{R_l} D_{n k}^J(\alpha\beta\gamma) |J \rangle_{n k} \tag{57}$$

We must compute how J split under a subduction $R_3 \supset \Gamma_1$. For instance, if $\Gamma_1 = T_d$, which is tetrahedral symmetry, and that we the splitting at $J = 2$, then the split is (E, T_2) . We build the corresponding wavefunction $(|2 \rangle_{-2}, |2 \rangle_1, |2 \rangle_0, |2 \rangle_1, |2 \rangle_2)$ and $(|E \rangle_1, |E \rangle_2, |T_2 \rangle_1, |T_2 \rangle_2, |T_2 \rangle_3)$ as outlined by Harter [3] for octahedral symmetry. From (56) we have,

$$|e \rangle = P_{ef}^E |J \rangle_{m k} / \sqrt{N^E}, \tag{58}$$

$$|t \rangle = P_{tu}^{T_1} |J \rangle_{m k} / \sqrt{N^{T_2}}. \tag{59}$$

The local symmetry of $C_2 = \{1, R_3^2\}$ has a projector P^{0_2} ,

$$P^{0_2} |2 \rangle_2 = \frac{1}{2} (1 + R_3^2) |2 \rangle_2 \tag{60}$$

We need the tetragonal ($T_d \supset D_{2d} \supset C_2$) projectors P_{ij}^α of T_d and only those for which $j = 0_2$. Thus, we find the induced representation $D^{0_2}(C_2) \uparrow T_d$ of T_d by performing a correlation between the character tables of C_v and T_d :

C_2	1	R_3^2
0_2	1	1
1	1	-1

(61)

Using columns 1 and I_1 of T_d table from (54) gives,

$$\begin{array}{c|cc}
 0_2(C_2) \uparrow T_d & 0_2 & 1_2 \\
 \hline
 A_1 & 1 & \cdot \\
 A_2 & \cdot & 1 \\
 E & 1 & 1 \\
 T_1 & 1 & 2 \\
 T_2 & 2 & 1
 \end{array} \tag{62}$$

$$\begin{array}{c|ccccc}
 T_d \uparrow D_{2d} & A_1 & A_2 & B_1 & B_2 & E \\
 \hline
 A_1 & 1 & \cdot & \cdot & \cdot & \cdot \\
 A_2 & \cdot & \cdot & 1 & \cdot & \cdot \\
 E & 1 & \cdot & 1 & \cdot & \cdot \\
 T_1 & \cdot & \cdot & \cdot & 1 & 1 \\
 T_2 & \cdot & 1 & \cdot & \cdot & 1
 \end{array} \tag{63}$$

It is clear from (62) that 0_2 correlates with the tetrahedral component E and T_2 . Therefore, we have $D^E(P^{0_2}) = \begin{pmatrix} 1 & \cdot \\ \cdot & 1 \end{pmatrix}$ and $D^{T_2}(P^{0_2}) = \begin{pmatrix} \cdot & \cdot & \cdot \\ \cdot & \cdot & \cdot \\ \cdot & \cdot & 1 \end{pmatrix}$. This tells us that we must use the third row of the tetragonal D-matrix for T_2 symmetry irrep, however, in the case of E symmetry irrep, it said both the first and third could be used. Therefore, consider D_{2d} and repeat correlation with T_d symmetry group, as shown by (63). We find that A_1 correlates with E and A_2 correlates with T_2 . Both suggest that the last rows in E and T_2 D-matrices are needed (57), depending on the D-function of R_3 and symmetry irreps coset leaders. Let's choose the following coset leaders. We can write each coset leader in terms of its Euler angle rotation. Figure 2. shows the Euler machine designed and built by Harter to perform these operations [3,14]. There are sequenced pivot bearings connecting each frame to its neighbor. One of the three Euler angles (α, β, γ) is displayed on each bearing's indicator and dial.

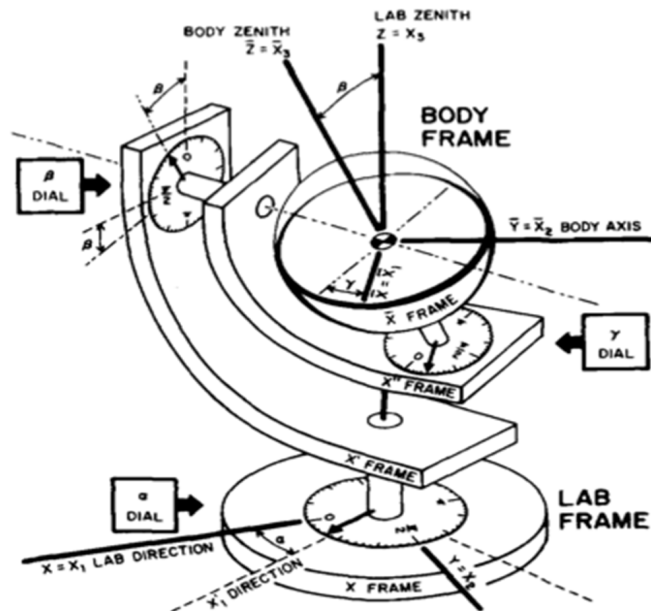


Figure 2. Schematic of Harter Euler machine. Euler angles as rotation position coordinates are defined [14]. There are four rigid frames that make up the Euler machine, each defining a coordinate axis and being supported by the others. The zeniths of the body and laboratory are shown in respective insets.

Harter [3] showed that the ordered rotation sequence of lab-based operations orients the body into position relative to the lab, i.e.,

$$R(\alpha 00)R(0\beta 0)R(00\gamma) = R(\alpha\beta\gamma). \tag{64}$$

There are steps we must perform to find $R(\alpha\beta\gamma)$. As shown in Figure 3, α is a rotation around the z-axis, β around y-axis, and γ rotation around z-axis. The first move is to zero the azimuth angle $R(-\phi 00)$ with the z-crank, and, then, zero the polar angle $R(0-\theta 0)$ with the crank, finally the ω rotation is given by the z crank $R(\omega 00)$. To complete this operation, we return ω to its original position by doing the reserve operation $R(\phi 00) R(0\theta 0)$. This allows us to create the expression between Euler rotations and Darboux rotations,

$$R(\phi 00) R(0\theta 0)R(\omega 00) R(0-\theta 0) R(-\phi 00) = R(\alpha 00) R(0\beta\beta 0)R(00\gamma) \tag{65}$$

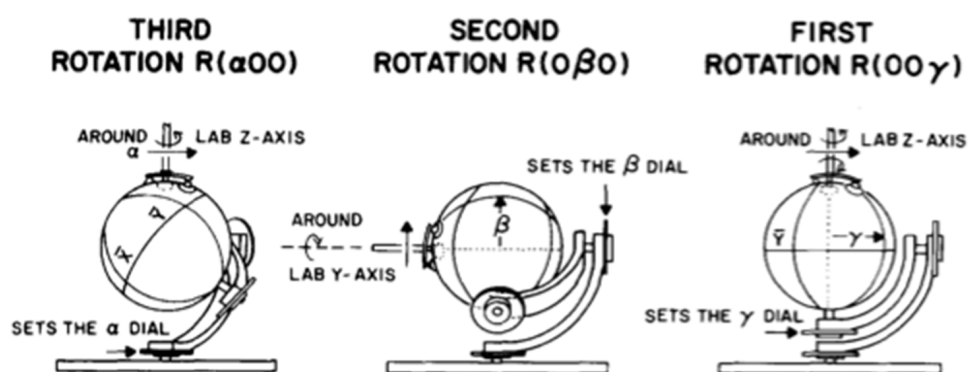


Figure 3. Rotation position of the three lab axes [3]. The ordered rotational sequence of lab-based operations orients the body into position relative to the lab.

We obtain the Euler angles from Darboux angles [2] as described by (66):

$$\begin{aligned} \cos(\alpha + \gamma/2)\cos(\beta/2) &= \cos(\omega/2), \\ \sin(\alpha + \gamma/2)\cos(\beta/2) &= \sin(\omega/2)\cos(\theta), \\ \cos(\alpha - \gamma/2)\sin(\beta/2) &= \sin(\omega/2)\sin(\theta)\sin(\phi), \\ \sin(\alpha - \gamma/2)\sin(\beta/2) &= \sin(\omega/2)\sin(\theta)\cos(\phi). \end{aligned} \tag{66}$$

Here we find all following for our coset leaders written in their polar form:

$$\begin{aligned} R_1 &= R(-\pi/2\pi/2\pi/2), R_1^3 = R(-\pi/2\pi/2\pi/2), R_2 = R(0\pi/20), \\ R_2^3 &= R(0-\pi/20), R_3^3 = R(0\pi\pi/2), \\ R_3 &= R(00\pi/2), i_1 = R(0\pi/4\pi), i_2 = R(\pi\pi/4\pi), i_3 = R(\pi/4\pi/2\pi), i_4 = R(-\pi/4\pi/2\pi), \\ i_5 &= R(3\pi/2\pi/4\pi), i_6 = R(\pi/2\pi/4\pi) \end{aligned} \tag{67}$$

We could have also us the follow alternative sets of cosets leaders:

$$\begin{aligned} 1 &= R(000), R_1^2 = R(-\pi/2\pi/2\pi), R_2^2 = R(0\pi/2\pi), R_3^2 = R(0\pi/2\pi), \\ r_1 &= R(-\pi/3\pi/32\pi/3), r_2 = R(\pi/3\pi/3 - 2\pi/3), r_3 = R(\pi/3 - \pi/3 - 2\pi/3), \\ r_4 &= R(-\pi/3 - \pi/32\pi/3), r_1^2 = R(-\pi/3\pi/3 - 2\pi/3), r_2^2 = R(\pi/3 - \pi/32\pi/3), r_3^2 \\ &= R(\pi/3 - \pi/32\pi/3), r_4^2 = R(-\pi/3\pi/3 - 2\pi/3) \end{aligned} \tag{68}$$

By using (66) we found the Euler representation (56) leading cosets:

$$\begin{aligned}
 R_1 &= R(-\pi/2\pi/2\pi/2), R_1^3 = R(-\pi/2\pi/2\pi/2), R_2 = R(0\pi/20), \\
 R_2^3 &= R(0 - \pi/20), R_3^3 = R(3\pi/40\pi/4), \\
 R_3 &= R(\pi/403\pi/4), i_1 = R(0\pi/2\pi), i_2 = R(3\pi/4\pi/20), i_3 = R(\pi/4\pi/23\pi/4), i_4 = R(3\pi/4\pi/2\pi/4), \\
 i_5 &= R(\pi/2\pi/2\pi/2), i_6 = R(\pi/2\pi/2\pi/2),
 \end{aligned}
 \tag{69}$$

Thus, we proceed with the example by finding the representation components of $\mathfrak{D}_{m_2}^2(\alpha\beta\gamma)$ for each coset leader by taking only the first column of the $\mathfrak{D}_{m_2}^2(\alpha\beta\gamma)$ matrix (49), therefore,

$$\mathfrak{D}_{m_2}^2(\alpha\beta\gamma) = \begin{pmatrix} e^{-i2(\alpha+\gamma)} \left(\frac{1+\cos\beta}{2}\right)^2 \\ e^{-i(\alpha+2\gamma)} \left(\frac{1+\cos\beta}{2}\right) \sin\beta \\ e^{-i2\gamma} \sqrt{\frac{3}{8}} (\sin\beta)^2 \\ e^{i(\alpha-2\gamma)} \left(\frac{1-\cos\beta}{2}\right) \sin\beta \\ e^{2i(\alpha-\gamma)} \left(\frac{1-\cos\beta}{2}\right)^2 \end{pmatrix}
 \tag{70}$$

We evaluate (70) for the coset leaders, and we have

$$\begin{aligned}
 \mathfrak{D}^2(R_3) &= \begin{pmatrix} 1 \\ 0 \\ 0 \\ 0 \\ 0 \end{pmatrix}, \mathfrak{D}^2(R_3^3) = \begin{pmatrix} 0 \\ 0 \\ 0 \\ 0 \\ 1 \end{pmatrix}, \mathfrak{D}^2(R_1) = \begin{pmatrix} 1/4 \\ -i/2 \\ -\sqrt{3}/8 \\ i/2 \\ 1/4 \end{pmatrix}, \mathfrak{D}^2(R_1^3) = \begin{pmatrix} 1/4 \\ i/2 \\ -\sqrt{3}/8 \\ -i/2 \\ 1/4 \end{pmatrix} \\
 \mathfrak{D}^2(R_2) &= \begin{pmatrix} 1/4 \\ 1/2 \\ \sqrt{3}/8 \\ 1/2 \\ 1/4 \end{pmatrix}, \mathfrak{D}^2(R_2^3) = \begin{pmatrix} 1/4 \\ -1/2 \\ \sqrt{3}/8 \\ -1/2 \\ 1/4 \end{pmatrix}, \mathfrak{D}^2(i_3) = \begin{pmatrix} \frac{1}{4} \\ \frac{1-i}{2\sqrt{2}} \\ -i\sqrt{\frac{3}{8}} \\ \frac{-1+i}{2\sqrt{2}} \\ \frac{1}{4} \end{pmatrix}, \mathfrak{D}^2(i_4) = \begin{pmatrix} \frac{1}{4} \\ -\frac{1-i}{2\sqrt{2}} \\ i\sqrt{\frac{3}{8}} \\ \frac{1-i}{2\sqrt{2}} \\ \frac{1}{4} \end{pmatrix} \\
 \mathfrak{D}^2(i_1) &= \begin{pmatrix} 1/4 \\ 1/2 \\ \sqrt{3}/8 \\ 1/2 \\ 1/4 \end{pmatrix}, \mathfrak{D}^2(i_2) = \begin{pmatrix} 1/4 \\ -1/2 \\ \sqrt{3}/8 \\ -1/2 \\ 1/4 \end{pmatrix}, \mathfrak{D}^2(i_5) = \begin{pmatrix} 1/4 \\ i/2 \\ -\sqrt{3}/8 \\ -i/2 \\ 1/4 \end{pmatrix}, \mathfrak{D}^2(i_6) = \begin{pmatrix} 1/4 \\ -i/2 \\ -\sqrt{3}/8 \\ i/2 \\ 1/4 \end{pmatrix}
 \end{aligned}
 \tag{71}$$

Now, we use Equation (54) through (71) to determine our orbital states (72).

$$\begin{aligned}
 \left| \begin{matrix} T_2 \\ 1 \end{matrix} \right\rangle &= \left(-\left| \begin{matrix} 2 \\ -1 \end{matrix} \right\rangle - \left| \begin{matrix} 2 \\ 1 \end{matrix} \right\rangle \right) / \sqrt{2} \\
 \left| \begin{matrix} T_2 \\ 2 \end{matrix} \right\rangle &= i \left(\left| \begin{matrix} 2 \\ -1 \end{matrix} \right\rangle + \left| \begin{matrix} 2 \\ 2 \end{matrix} \right\rangle \right) / \sqrt{2} \\
 \left| \begin{matrix} T_2 \\ 3 \end{matrix} \right\rangle &= \left(-\left| \begin{matrix} 2 \\ -2 \end{matrix} \right\rangle + \left| \begin{matrix} 2 \\ 2 \end{matrix} \right\rangle \right) / \sqrt{2} \\
 \left| \begin{matrix} E \\ 1 \end{matrix} \right\rangle &= \left| \begin{matrix} 2 \\ 0 \end{matrix} \right\rangle \\
 \left| \begin{matrix} E \\ 2 \end{matrix} \right\rangle &= \left(\left| \begin{matrix} 2 \\ -2 \end{matrix} \right\rangle + \left| \begin{matrix} 2 \\ 2 \end{matrix} \right\rangle \right) / \sqrt{2}
 \end{aligned}
 \tag{72}$$

By applying spherical harmonics, we have,

$$\begin{aligned}
 n_2 \left\langle \theta\phi \left| \begin{matrix} 2 \\ 2 \end{matrix} \right\rangle &= n_2 Y_2^2(\theta\phi) = \sqrt{\frac{3}{8}} e^{2i\phi} \sin^2\theta = \sqrt{\frac{3}{8}} (x + iy)^2 / r^2 \\
 n_2 \left\langle \theta\phi \left| \begin{matrix} 2 \\ 1 \end{matrix} \right\rangle &= n_2 Y_1^2(\theta\phi) = \sqrt{\frac{3}{8}} e^{i\phi} \sin^2\theta = \sqrt{\frac{3}{8}} (x + iy) / r^2 \\
 n_2 \left\langle \theta\phi \left| \begin{matrix} 2 \\ 0 \end{matrix} \right\rangle &= n_2 Y_0^2(\theta\phi) = (3\cos^2\theta - 1) / 2 = (2z^2 - x^2 - y^2) / 2r^2 \\
 n_2 \left\langle \theta\phi \left| \begin{matrix} 2 \\ -1 \end{matrix} \right\rangle &= n_2 Y_{-1}^2(\theta\phi) = -\sqrt{\frac{3}{2}} e^{-i\phi} \sin\theta \cos\theta = -\sqrt{\frac{3}{2}} (x - iy)z / r^2 \\
 n_2 \left\langle \theta\phi \left| \begin{matrix} 2 \\ -2 \end{matrix} \right\rangle &= n_2 Y_{-2}^2(\theta\phi) = \sqrt{\frac{3}{8}} e^{-2i\phi} \sin^2\theta = \sqrt{\frac{3}{8}} (x - iy)^2 / r^2
 \end{aligned} \tag{73}$$

By combining (72) and (73), we acquire the same result for the rotational tensor given in [3].

B. Vibrational Wavefunction

Consider the vibration Hamiltonian expanded in terms of raising a^\dagger and lowering a operators,

$$H = \sum_{\alpha} \sum_i \left(\alpha_i^{\alpha\dagger} \alpha_i^{\alpha} + \frac{1}{2} \right). \tag{74}$$

Suppose ϵ is an eigenstate of H then

$$H|\epsilon\rangle = \epsilon|\epsilon\rangle, \tag{75}$$

as such:

$$|\epsilon\rangle = \left| \dots n_i^{\alpha} \dots n_j^{\beta} \dots \right\rangle = \dots \left(a_i^{\alpha\dagger} \right)^{n_i^{\alpha}} \dots \left(a_j^{\beta} \right)^{n_j^{\beta}} |0 \dots\rangle / \sqrt{N}. \tag{76}$$

Furthermore, ν_i is the spectroscopy notation for Γ , such that in methane ν_1 for A_1 , ν_2 for E , ν_3 for T_2 , ν_4 for T_2 . There, E label ($2\nu_2$) has a triple degenerate:

$$\left| \dots n_1^E, n_2^E \dots (2\nu_2) \right\rangle = \left| \dots 2, 0 \dots (2\nu_2) \right\rangle, \left| \dots 1, 1 \dots (2\nu_2) \right\rangle, \left| \dots 0, 2 \dots (2\nu_2) \right\rangle. \tag{77}$$

(77) is exactly the same as Alvarez-Bajo et al. [10], i.e., $|V; \nu\rangle$, therefore, we can say

$$\left| V; \Psi_{vib}^{p, \Gamma_2, \gamma_2} \right\rangle = \sum_v D_v^{p, \Gamma_2, \gamma_2} |V; \nu\rangle_p \tag{78}$$

4. Concrete Example: Symmetry Analysis of Methane

The chemical formula for methane is CH_4 ; there are four hydrogen atoms bonded to one carbon atom. The ground state methane (CH_4) molecule has T_d symmetry, i.e., tetrahedral point group symmetry. Imagine a cube that has four hydrogen atoms placed at four of its corners laying diagonally at equal distances with a carbon atom at the center. These atoms are connected to each other via springs. Thus, the tetrahedral symmetry is shown in Figure 4.

The position of Hydrogen atoms or Y atoms will be represented with symmetry coordinates. Figure 4. shows a set of bases for the Y atoms. We will use these base sets to do the symmetry analysis of XY_4 . The vibrational modes will be calculated, and they can be simulated on a computer to understand the dynamics of XY_4 molecules better.

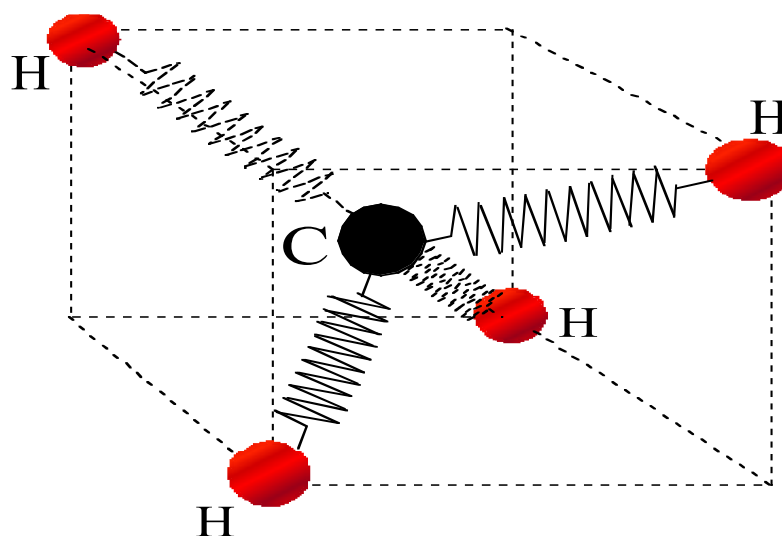


Figure 4. Diagrammatic illustration of a CH_4 molecule. This molecule has a tetrahedral symmetry. CH_4 belongs to a general class of molecules represented by XY_4 .

There are twelve bases stated describing the Y atom in XY_4 and three bases stated for the X atom. Bases set of Y atoms in Figure 4. are labeled by set selected symmetry operators in Figure 5,

$$\left\{ |A\rangle, |r_1A\rangle, |r_1^2A\rangle, |R_1^2A\rangle, |r_4A\rangle, |r_2^2A\rangle, |R_2^2A\rangle, |r_2A\rangle, |r_3^2A\rangle, |R_3^2A\rangle, |r_3A\rangle, |r_3^2\rangle \right\} \quad (79)$$

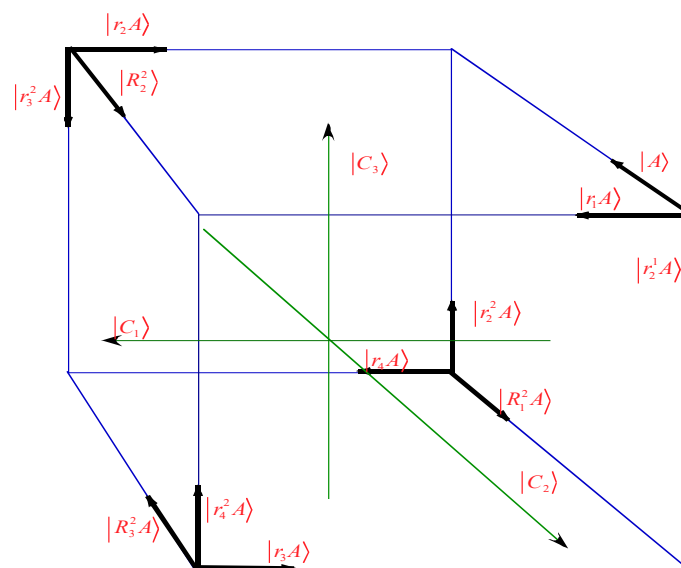


Figure 5. Symmetry coordinates for the XY_4 molecule. Displayed on each of the atoms are the symmetry bases.

The symmetry operations for an object with T_d symmetry is given by the following in Figure 6.

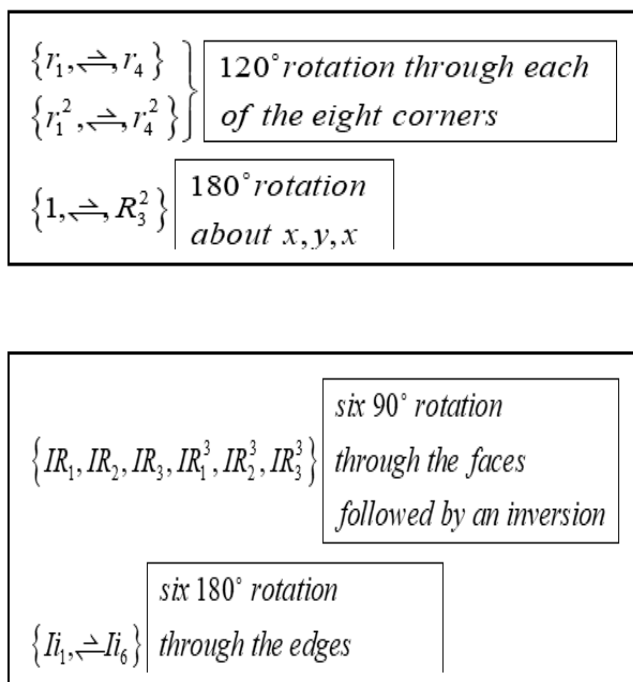


Figure 6. Symmetry operations for the T_d point group. 24 symmetry operations are displayed for four different axes of rotations.

Although (a) and (b) make up T_d point symmetry, the symmetry operations of (a) moves the four Y atoms to the same place that the symmetry operations in (b) would. Consequently, the symmetry operation in (a) and (b) of the two cosets of twelve in T_d base vectors of the X atom are,

$$\{|C_1\rangle, |C_2\rangle, |C_3\rangle\} \tag{80}$$

The eigenvectors are then obtained from the group projectors P_{jk}^α . When the particular symmetry is known, the eigenvectors or near-eigenvectors $|e_{jk}^\alpha A\rangle$ are very easily found,

$$|e_{jk}^\alpha A\rangle = \frac{P_{jk}^\alpha |A\rangle}{\sqrt{N_k^\alpha}} \tag{81}$$

There exists a local symmetry of $C_v = \{1, \sigma\}$ that preserves each coordinate vector $|rA\rangle$ so $(\sigma|rA) = |rA\rangle$. It has a projector P^{0_2} ,

$$P^{0_2} = \frac{1}{2}(1 + \sigma)|A\rangle. \tag{82}$$

Thus, it spans an induced representation $D^{0_2}(C_v) \uparrow T_d$ of T_d . The full T_d labeled orbit is given by a 12-dimensional induced representation $D^{0_2}(C_v) \uparrow T_d$. The character tables of C_v ,

C_v	1	σ
0_2	1	1
1	1	-1

(83)

T_d	1	$(r_1 \dots r_1^2 \dots)$	$(R_1^2 \dots)$	$(IR_1 \dots IR_3^3 \dots)$	$(Ii_1 \dots)$
A_1	1	1	1	1	1
A_2	1	1	1	-1	-1
E	2	-1	2	0	0
T_1	3	0	-1	1	-1
T_2	3	0	-1	-1	1

(84)

and T_d and using columns 1 and Ii_1 of T_d table gives (63). However, by considering the sub-group chain $T_d \supset C_{3v} \supset C_v$, we find the symmetry characteristic of the energy levels in XY_4 as shown by Figure 5. We start with the C_{3v} character table:

$$\begin{array}{c|ccc}
 C_{3v} & 1 & (r, r^2) & (\sigma_1, \sigma_2, \sigma_3) \\
 \hline
 A_1 & 1 & 1 & 1 \\
 A_2 & 1 & 1 & -1 \\
 E & 2 & -1 & 0
 \end{array} \tag{85}$$

Then, we determine the correlation $T_d \supset D_3 : T_d \uparrow D_3$ between the T_d character table (60) and the C_{3v} character table (85),

$$\begin{array}{c|ccc}
 T_d \uparrow C_{3v} & A_1 & A_2 & E \\
 \hline
 A_1 & 1 & . & . \\
 A_2 & . & 1 & . \\
 E & . & . & 1 \\
 T_1 & . & 1 & 1 \\
 T_2 & 1 & . & 1
 \end{array} \tag{86}$$

Next, we obtain the correlation between C_{3v} and C_v ,

$$\begin{array}{c|cc}
 D_3 \uparrow C_v & 0_2 & 1_2 \\
 \hline
 A_1 & 1 & . \\
 A_2 & . & 1 \\
 E & 1 & 1
 \end{array} \tag{87}$$

$$\Rightarrow D^{0_2} \uparrow T_d = A_1 \oplus E \oplus T_1 \oplus 2T_2 \oplus \tag{88}$$

From (79)–(88), we construct the following energy level correlation diagram (see Figure 7), which shows symmetry splitting for the subgroup chain $T_d \supset C_{3v} \supset C_v$. This gives the eigenvectors:

$$\begin{aligned}
 |e_j^\alpha\rangle &= P_{ij}^\alpha |A\rangle = \frac{1}{\sqrt{G}} \sum_g D_{ij}^{\alpha*}(g) |gA\rangle, \\
 \text{where } \alpha &= A_1, E, T_1, T_2
 \end{aligned} \tag{89}$$

$$\left\{ \begin{array}{l}
 |e_1^{A_1}\rangle = \frac{1}{\sqrt{24}} \sum_g D_{11}^{A_1}(g) |gA\rangle, \\
 |e_j^E\rangle = \frac{1}{\sqrt{24}} \sum_g D_{j1}^E(g) |gA\rangle, \quad j = 1, 2, \\
 |e_j^{T_1}\rangle = \frac{1}{\sqrt{8}} \sum_g D_{j1}^{T_1}(g) |gA\rangle, \quad j = 1, 2, 3, \\
 |e_j^{T_2}\rangle = \frac{1}{\sqrt{8}} \sum_g D_{j1}^{T_2}(g) |gA\rangle, \quad j = 1, 2, 3, \quad |e_j^{T_2}\rangle = \frac{1}{\sqrt{8}} \sum_g D_{j3}^{T_2}(g) |gA\rangle, \quad j = 1, 2, 3
 \end{array} \right. \tag{90}$$

Irrep matrix D^{Γ_1} are determined from irrep idempotent $P_j^{\Gamma_1}$ by constructing the normalize element $P_j^{\Gamma_1} g P_j^{\Gamma_1}$. In Appendix A we list the trigonal and tetrahedral bases 3×3 and 2×2 matrices. We demonstrate in Section 2 how to compute D^{Γ_1} for 2×2 matrices, however, for more details consult red. 3. In (89) the element of D^{Γ_1} are used to find the eigenvectors.

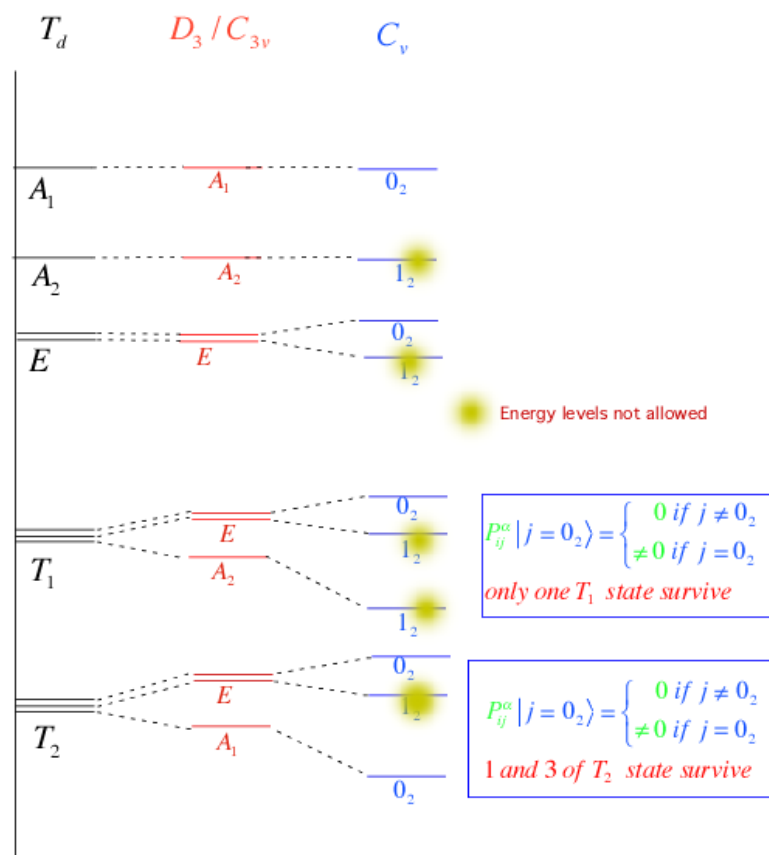


Figure 7. The level splitting diagram shows the level of correlations for the subgroup chain $T_d \supset C_{3v} \supset C_v$. The level splitting of the T_d irreps is reduced to one of its subgroups which is further reduced. The levels split according to the way their corresponding class of idempotent split.

The projected near eigenvectors corresponding to $T_d \supset C_{3v} \supset C_v$ are given below,

	$ e^{A_1}\rangle$	$ e^{E_1}\rangle$	$ e^{E_2}\rangle$	$ e^{T_{11}}\rangle$	$ e^{T_{12}}\rangle$	$ e^{T_{13}}\rangle$	$ e^{T_{21}}\rangle$	$ e^{T_{22}}\rangle$	$ e^{T_{23}}\rangle$	$ e^{T_{31}}\rangle$	$ e^{T_{32}}\rangle$	$ e^{T_{33}}\rangle$
$ 1\rangle$	1	2	0	2	0	0	3	0	0	0	0	2
$ r_1\rangle$	1	-1	1	-1	-3	0	3	0	0	0	3	-1
$ r_1^2\rangle$	1	-1	-1	-1	3	0	3	0	0	0	-3	-1
$ R_1^2\rangle$	1	2	0	0	2	1	-1	-1	-1	1	-2	0
$ r_4\rangle$	1	-1	1	1	-1	1	-1	2	0	1	1	1
$ r_2^2\rangle$	1	-1	-1	-1	-1	1	-1	-1	-1	1	1	-1
$ R_2^2\rangle$	1	2	0	0	2	-1	-1	-1	-1	1	2	0
$ r_2\rangle$	1	-1	1	-1	1	-1	-1	-1	1	1	-1	-1
$ r_3^2\rangle$	1	-1	-1	1	1	-1	-1	2	0	1	-1	1
$ R_3^2\rangle$	1	2	0	-2	0	0	-1	2	0	0	0	-2
$ r_3\rangle$	1	-1	1	1	3	0	-1	-1	-1	0	-3	1
$ r_4^2\rangle$	1	-1	-1	1	-3	0	-1	-1	-1	0	3	1
	$2\sqrt{3}$	$2\sqrt{6}$	$2\sqrt{2}$	4	$4\sqrt{3}$	$\sqrt{6}$	6	$2\sqrt{6}$	$2\sqrt{2}$	$\sqrt{6}$	$4\sqrt{3}$	4

(91)

The T_1 and T_2 eigenvectors are written in the trigonal bases (see Appendices A.4–A.6) and are related to the subgroup chain $T_d \supseteq D_{2d} \supseteq C_v$ by the unitary transformation,

$$T = \begin{pmatrix} \frac{1}{\sqrt{2}} & \frac{-1}{\sqrt{2}} & 0 \\ \frac{1}{\sqrt{6}} & \frac{1}{\sqrt{6}} & \frac{-2}{\sqrt{6}} \\ \frac{1}{\sqrt{3}} & \frac{1}{\sqrt{3}} & \frac{1}{\sqrt{3}} \end{pmatrix} \tag{92}$$

Applying the transformation to the irrep matrices of the $T_d \supset C_{3v} \supset C_v$ chain gives the irrep matrices for the $T_d \supseteq D_{2d} \supseteq C_v$ chain (see Appendices A.1–A.3). As a result, we find the eigenvectors in a new bases which is given by,

	$ e^{A_1}\rangle$	$ e^{E_1}\rangle$	$ e^{E_2}\rangle$	$ e^{T_1}_{11}\rangle$	$ e^{T_1}_{12}\rangle$	$ e^{T_1}_{13}\rangle$	$ e^{T_2}_{11}\rangle$	$ e^{T_2}_{12}\rangle$	$ e^{T_2}_{13}\rangle$	$ e^{T_2}_{31}\rangle$	$ e^{T_2}_{32}\rangle$	$ e^{T_2}_{33}\rangle$
$ 1\rangle$	1	2	0	1	-1	0	1	0	0	0	0	1
$ r_1\rangle$	1	-1	1	0	1	-1	0	1	0	1	0	0
$ r_1^2\rangle$	1	-1	-1	-1	0	1	0	0	1	0	1	0
$ R_1^2\rangle$	1	2	0	1	1	0	1	0	0	0	0	-1
$ r_4\rangle$	1	-1	1	0	-1	1	0	-1	0	-1	0	0
$ r_2^2\rangle$	1	-1	-1	-1	0	-1	0	0	-1	0	-1	0
$ R_2^2\rangle$	1	2	0	-1	-1	0	-1	0	0	0	0	-1
$ r_2\rangle$	1	-1	1	0	1	1	0	1	0	-1	0	0
$ r_3^2\rangle$	1	-1	-1	1	0	-1	0	0	-1	0	1	0
$ R_3^2\rangle$	1	2	0	-1	1	0	-1	0	0	0	0	1
$ r_3\rangle$	1	-1	1	0	-1	-1	0	-1	0	1	0	0
$ r_4^2\rangle$	1	-1	-1	1	0	1	0	0	1	0	-1	0
	$2\sqrt{3}$	$2\sqrt{6}$	$2\sqrt{2}$	$2\sqrt{2}$	$2\sqrt{2}$	$2\sqrt{2}$	2	2	2	2	2	2

In Figure 8, we display all the genuine vibrations of XY_4 . Now, we consider the energy eigenvalues using those bases for XY_4 molecule.

4.1. Solving the Equation of Motion

From the T_d symmetry projection operators, we can construct the eigenstates and use them to partially solve the equation of motion (94),

$$m|\ddot{x}\rangle = -F|x\rangle \tag{94}$$

The number of elements we need for the force matrix is considerably less than $(15)^2 = 225$ due to symmetry considerations. Only 18 elements are needed for the force matrix. Because of the non-genuine vibration of the T_2 mode, it will acquire in general (82), which simplifies to a block matrix form (96). To compute the F-matrix we must obtain the component $\langle i|F|j\rangle$ by computing the product of the projections of each spring on the coordinate axis $x_i = \langle i|x\rangle$ and $x_j = \langle j|x\rangle$ for all spring and summing products.

$$-F_1 = \langle 1|F|1\rangle\langle 1|x\rangle + \langle 1|F|2\rangle\langle 2|x\rangle + \langle 1|F|3\rangle\langle 3|x\rangle + \dots, \tag{95}$$

which implies a force matrix given by,

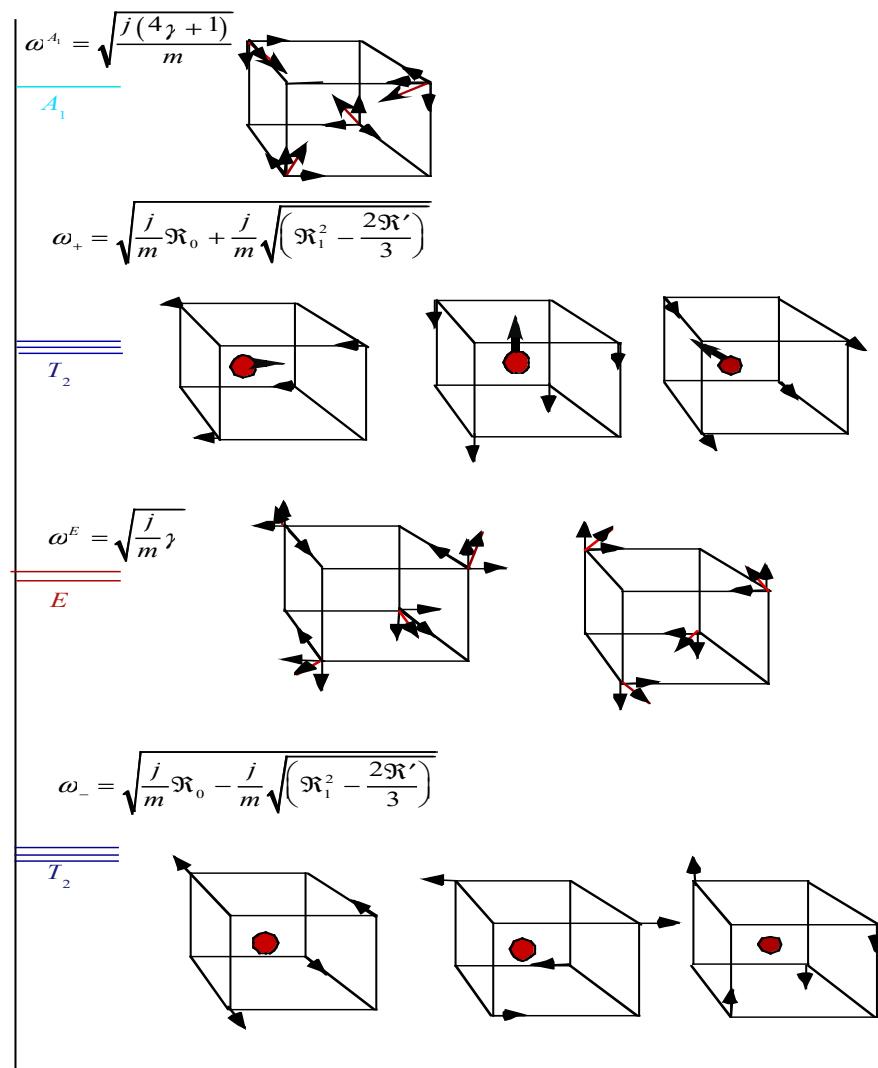


Figure 8. The XY_4 vibrational modes and spectra. Each mode shows the movement of X atoms and Y atoms and their corresponding energies. A_1 is the squeezing mode. Two T_2 modes for the H atoms, one for the C atom, and two vibrational modes are mixed with one translation mode. The E-mode is similar to a breathing mode.

$$\begin{matrix} |A\rangle \\ |C_1\rangle \end{matrix} \begin{bmatrix} |1\rangle & |2\rangle & |3\rangle & |4\rangle & |5\rangle & |6\rangle & |7\rangle & |8\rangle & |9\rangle & |10\rangle & |11\rangle & |12\rangle & |13\rangle & |14\rangle & |15\rangle \\ k + \frac{j}{3} & k + \frac{j}{3} & k + \frac{j}{3} & \frac{k}{2} & \bullet & \frac{k}{2} & \frac{k}{2} & \frac{k}{2} & \bullet & \bullet & \bullet & \bullet & -\frac{j}{3} & -\frac{j}{3} & -\frac{j}{3} \\ & & & & & & & & & & & & \frac{4j}{3} & \bullet & \bullet \end{bmatrix} \quad (96)$$

$$\begin{matrix} |A\rangle \\ |C_1\rangle \end{matrix} \begin{bmatrix} |1\rangle & |2\rangle & |3\rangle & |4\rangle & |5\rangle & |6\rangle & |7\rangle & |8\rangle & |9\rangle & |10\rangle & |11\rangle & |12\rangle & |13\rangle & |14\rangle & |15\rangle \\ m & \bullet \\ \bullet & M & \bullet & \bullet \end{bmatrix} \quad (97)$$

Notice in the force matrix, only the first column must be written down. Thus, with our eigenvectors applied to this first row we obtain the eigenfrequencies:

$$(\omega^\alpha)^2 = \langle m^{-1}F \rangle = \frac{1}{m} \sum_g \langle A|F|gA \rangle D_{ij}^\alpha(g) \quad (98)$$

where $\alpha = A_1, E, T_1, T_2$

$$A_1 \text{ mode } \omega^{A_1} = \sqrt{\frac{4k + j}{m}} \tag{99}$$

$$E\text{-mode } \omega^E = \sqrt{\frac{2k}{m}}. \tag{100}$$

T_1 mode has an eigenfrequency of zero corresponding to a pure classical rotation. Since XY_4 is spherically symmetric, the following rotational Hamiltonian can describe T_1 modes (see Figure 9),

$$H_r = \frac{J^2}{2I}. \tag{101}$$

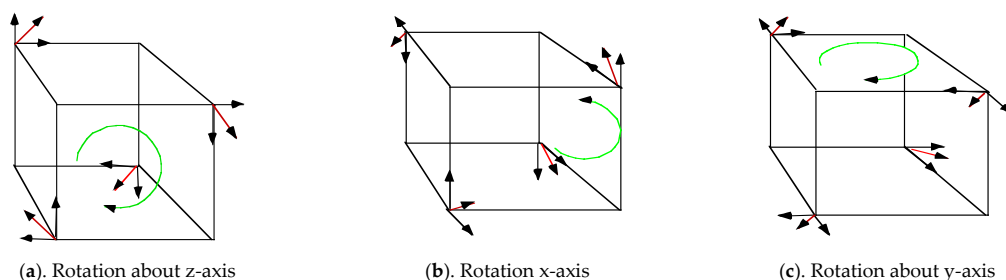


Figure 9. The T_1 modes of XY_4 is a pure rotation.

4.2. Non-Genuine Vibration

There are two T_2 modes for the H atoms and one for the C atom. Thus, there are six eigenfrequencies since the dimension of T_2 is three (see Figure 8). The T_2 are not all genuine vibrations, but two vibrational modes are mixed with one translation mode. By using the above T_2 eigenvectors and the $|C\rangle$ bases to transform each Q matrix where $Q = F$ or $Q = m$, we acquire a block diagonal form,

$$\begin{bmatrix} \langle T_2 | Q | T_2 \rangle & \langle T_2 | Q | T_2 \rangle & \langle T_2 | Q | C_j \rangle \\ \langle T_2 | Q | T_2 \rangle & \langle T_2 | Q | T_2 \rangle & \langle T_2 | Q | C_j \rangle \\ \langle C_j | Q | T_2 \rangle & \langle C_j | Q | T_2 \rangle & \langle C_j | Q | C_j \rangle \end{bmatrix} \tag{102}$$

Note, there are nine eigenvalues and one for each $j = 1, 2, 3$ three 3×3 Γ -matrices, since by symmetry each 3×3 matrix is the same. By solving one of them we determine all nine eigenvalues of three triply degenerate levels. (103) gives the matrix element calculation for (102),

$$\langle T_2 | Q | T_2 \rangle = \langle A | P_{j1}^{T_2} Q P_{j1}^{T_2} | A \rangle = \sum_g \langle A | Q | g A \rangle D_{11}^{T_2}(g), \tag{103}$$

$$\langle T_2 | Q | T_2 \rangle = \sum_g \langle A | Q | g A \rangle D_{33}^{T_2}(g), \tag{104}$$

$$\langle T_2 | Q | T_2 \rangle = \langle T_2 | Q | T_2 \rangle = \sum_g \langle A | Q | g A \rangle D_{13}^{T_2}(g), \tag{105}$$

$$\langle T_2 | Q | C_j \rangle = \langle T_2 | Q | C_j \rangle = \langle A | Q P_{1j}^{T_2} | C_j \rangle, \tag{106}$$

$$\langle T_2 | Q | C_j \rangle = \langle T_2 | Q | C_j \rangle = \langle A | Q P_{1j}^{T_2} | C_j \rangle, \tag{107}$$

$$\langle C_j | Q | C_j \rangle = \langle C_j | Q | C_j \rangle. \tag{108}$$

First, we consider $Q = F$ in (102) to give the force matrix as

$$\begin{bmatrix} 2(\gamma + 1/3) & \frac{1}{3} & \frac{-2}{3} \\ \frac{1}{3} & \frac{1}{3} & \frac{-2}{3} \\ \frac{-2}{3} & \frac{-2}{3} & \frac{4}{3} \end{bmatrix}, \quad \gamma = \frac{k}{j}. \tag{109}$$

Next, by making $Q = m$ in (103) through (107) and $Q = M$ to give,

$$Q = mass \Rightarrow \begin{bmatrix} m & \bullet & \bullet \\ \bullet & m & \bullet \\ \bullet & \bullet & M \end{bmatrix}. \tag{110}$$

As a result, we have the following acceleration matrix,

$$\frac{j}{m} \begin{bmatrix} 2(\gamma + 1/3) & \frac{1}{3} & \frac{-2}{3} \\ \frac{1}{3} & \frac{1}{3} & \frac{-2}{3} \\ \frac{-2}{3}\alpha & \frac{-2}{3}\alpha & \frac{4}{3}\alpha \end{bmatrix}, \quad \gamma = \frac{k}{j}, \quad \alpha = \frac{m}{M}; \tag{111}$$

We solved the eigenvalue equation,

$$\lambda \left(\lambda^2 - 2 \left(\gamma + \frac{1}{2} + \frac{2}{3}\alpha \right) \lambda + \frac{2\gamma}{3} (4\alpha + 1) \right) = 0. \tag{112}$$

Solving (112), we have following eigenvalues

$$\begin{aligned} \lambda_0 &= 0; \\ \lambda_{\pm} &= \Re_0 \pm \sqrt{\left(\Re_1^2 - \frac{2\Re'}{3} \right)}, \end{aligned} \tag{113}$$

$$\begin{aligned} \text{where } \omega_{\pm} &= \sqrt{\frac{j}{m} \lambda_{\pm}} \\ \Re_0 &= \gamma + \frac{2}{3}\alpha + \frac{1}{2} \\ \Re_1 &= \gamma + \frac{2}{3}\alpha + \frac{1}{2} \\ \Re' &= \gamma - \frac{4}{3}\alpha + \frac{1}{6} \end{aligned} \tag{114}$$

The corresponding eigenvectors can be written as

$$|\lambda_0\rangle = \begin{bmatrix} 0 \\ 2 \\ 1 \end{bmatrix} \tag{115}$$

$$|\lambda_+\rangle = \begin{bmatrix} \frac{(\Re_1 + \sqrt{\Omega})}{4\alpha} \\ -\frac{1}{2\alpha} \\ 1 \end{bmatrix}, \tag{116}$$

$$|\lambda_-\rangle = \begin{bmatrix} \frac{-(\Re_1 + \sqrt{\Omega})}{4\alpha} \\ -\frac{1}{2\alpha} \\ 1 \end{bmatrix}, \tag{117}$$

$$\text{where } \Omega = \left(\Re_1^2 - \frac{2\Re'}{3} \right). \tag{118}$$

This procedure could be carried out using 2×2 matrices instead of 3×3 matrices since one of the T_2 modes is a pure translation. By excluding that mode, we only need to

solve a 2×2 matrix. For the translation, both the X atom and the four Y atoms should move by the same amount. As a result, we have,

$$|T_{2j}^{Trans}\rangle = 2|T_{2j3}\rangle + |C_j\rangle. \tag{119}$$

We illustrate $|T_{2j}^{Trans}\rangle$ in Figure 10 where the translation of H atoms or the Y atoms and X-atom for states that are in the $|C_1\rangle$ direction.

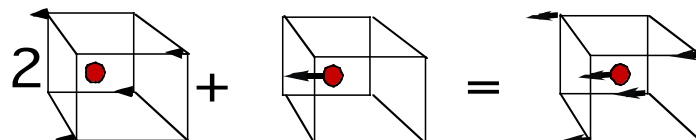


Figure 10. A T_2 translation mode resulting from the non-genuine T_2 mode. The motion of the Y atom is displayed in the left-most box, and the X atom is in the second box (middle), which combine to give the right-most box.

The translational mode and two vibrational modes of T_2 are now isolated (see Figure 10). This was achieved by taking linear combinations of the T_2 modes.

A T_2 mode that is orthogonal to (95) must be a genuine vibration, i.e.,

$$|T_{2j}^{vib}\rangle = 2M|T_{2j}\rangle - 4m|C_j\rangle. \tag{120}$$

(120) gives the genuine vibration from the non-genuine vibrations. We illustrate (120) pictorially in Figure 11.

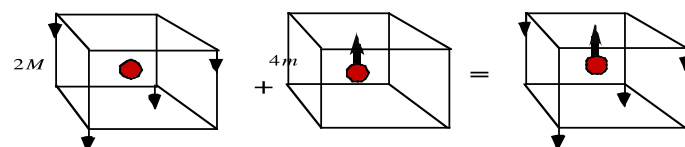


Figure 11. The genuine mode for $|T_{2j}^{vib}(\omega_-)\rangle$. The movement of the Y-atoms are opposite to the movement of the X-atoms.

We just need to find the overlap matrix between the next T_2 mode, namely $|T_{2j1}\rangle$, and $|T_{2j1}^{vib}\rangle$, i.e.,

$$\begin{pmatrix} \langle T_{2j1} | Q | T_{2j1}^{vib} \rangle & \langle T_{2j1} | Q | T_{2j}^{vib} \rangle \\ \langle T_{2j}^{vib} | Q | T_{2j1} \rangle & \langle T_{2j}^{vib} | Q | T_{2j}^{vib} \rangle \end{pmatrix} = \frac{j}{m} \begin{pmatrix} \frac{2(\gamma + \frac{1}{3})}{3} & \frac{2(M+4m)}{3} \\ \frac{1}{6M} & \frac{(M+4m)}{3M} \end{pmatrix}, \tag{121}$$

with eigenvalues,

$$\omega_{\pm} = \sqrt{\frac{j}{m} \Re_0 \pm \frac{j}{m} \sqrt{\left(\Re_1^2 - \frac{2\Re'}{3}\right)}}, \tag{122}$$

and the eigensolution

$$|e_j^{T_2}(\pm)\rangle = \epsilon_{\pm} |T_{2j1}\rangle + |T_{2j}^{vib}\rangle, \tag{123}$$

$$\text{where } \varepsilon_{\pm} = 6M \left(\mathfrak{R}_1 \pm \sqrt{\mathfrak{R}_1^2 - \frac{2}{3}\mathfrak{R}'} \right). \tag{124}$$

Figure 12 shows how the frequency of vibration is affected as the ratio of the spring coupling increases.

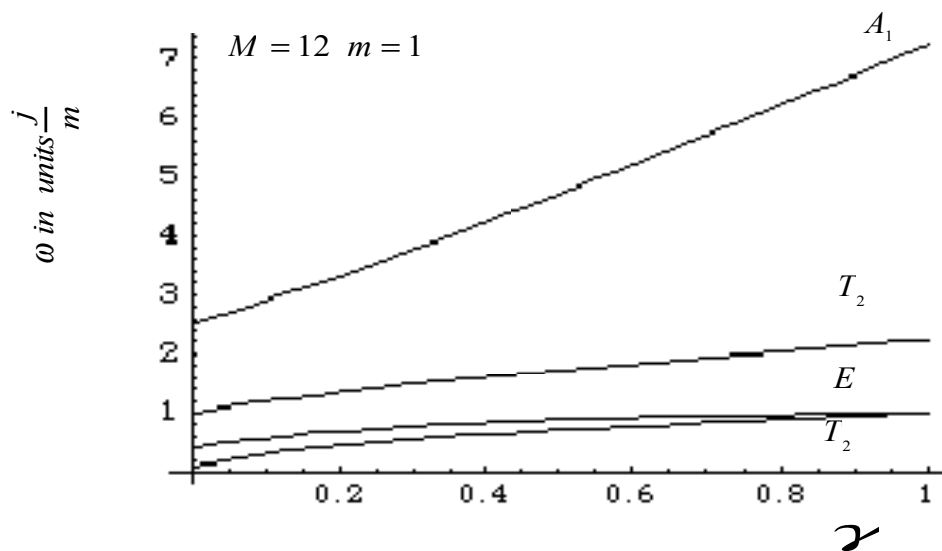


Figure 12. CH₄ vibration spectra with increasing spring ratio. The plot shows eigenvalues ω as function of the ratio k/j .

For the CH₄ molecular parameters values $m = 1, M = 12, k = 0.6,$ and $j = 2.66,$ (113) gives the following acceleration,

$$\begin{bmatrix} 2.97 & 28.37 \\ 0.04 & 1.18 \end{bmatrix}. \tag{125}$$

where we found the eigenvalues to be $\omega_+ = 3.44; \omega_- = 0.72$ and the eigenvectors of the vibration for the T_2 mode are,

$$\begin{aligned} |e_j^{T_2}(+)\rangle &= \begin{vmatrix} T_2 \\ j1 \end{vmatrix} + 0.02 \begin{vmatrix} T_2 \\ j \end{vmatrix} \text{ vib} \\ |e_j^{T_2}(-)\rangle &= -\begin{vmatrix} T_2 \\ j1 \end{vmatrix} + 0.08 \begin{vmatrix} T_2 \\ j \end{vmatrix} \text{ vib} \end{aligned} \tag{126}$$

Table 1 shows the observed with the computed in units of cm^{-1} . A_1 mode, and two T_2 modes compare with observed frequency. We obtain computed frequency by using the force constants of $j, k 5.495 \text{ aJA}^{-2},$ and $0.124 \text{ aJA}^{-2},$ respectively. However, the E-mode does not compare well.

Table 1. Frequency comparison.

XY_4 Irreps	Observed (cm^{-1})	Computed (cm^{-1})
A_1	2914.2	3179.8
E	1526.0	647.0
T_1	3020.3	3023.3
T_2	1306.3	1258.1

In the analysis of $XY_4,$ we see that only the T_2 moves the X atom. This means there is a coupling between the X and Y atoms through the j spring. It is evident that this is the case since the T_2 modes repel each other, as shown in Figure 12. In Figure 12, there is a clustering of (E, T_2) modes which is more pronounced when the strength of the j spring and mass ratio of

X and Y atom increases. For better results with the XY_4 molecule, we would need to consider bending forces for a more precise agreement.

5. Conclusions

It is possible to define every molecule according to its symmetry, or lack thereof, which can be expressed in terms of symmetry elements. The Projection Operator Technique utilizes the extended character table which includes each symmetry operation separately. We have demonstrated the power of the projector method to perform molecular calculations. As an example, a CH_4 molecule was considered for its tetrahedral symmetry, and our compute frequencies A_1 and the two T_2 's modes were in range of the observed values. By exploiting a molecule's symmetry, it is not necessary to solve the Schrödinger equation in detail.

Funding: This research received no external funding.

Data Availability Statement: Not Applicable.

Conflicts of Interest: The author declares no conflict of interest.

Appendix A.

If you perform a geometric symmetry operation on a particle located at position x,y,z and then apply one of the geometrical symmetry operations R , what are the new coordinates of the particle?

$$\begin{bmatrix} x' \\ y' \\ z' \end{bmatrix} = [D(R)] \begin{bmatrix} x \\ y \\ z \end{bmatrix} \quad (A1)$$

where the matrices $D(R)$ for each point group operation R . In the tetrahedral symmetry R is given by Figure 6. Moreover, assuming a fixed convention of rotating particles through an angle $-2\pi/n$ in the direction of u by defining $C_n(u)$ as a rotation of the particle (active operation) and determining the sign of the rotation by using the right-hand thumb rule, we find that the new coordinates for the particle are given as functions of the old coordinates. The irrep matrices $D(R)$ may be derived from the irreducible idempotents $P_j^{T_1}$ by constructing the guarded elements $P_i^{T_1} g P_j^{T_1}$, normalizing them, and using the elementary operation relation $P_i^{T_1} g P_j^{T_1} = D_{ij}^{T_1}(g) P_{ij}^{T_1}$. For example, let's consider the irrep $D^{T_{1u}}$ which represents the effects of O_h transformation on Cartesian unit vectors $\{\hat{x} = \hat{x}_1, \hat{y} = \hat{x}_2, \hat{z} = \hat{x}_3\}$. The effect of Ir_1 transformed the unit vector x_1 as

$$Ir_1|x_1\rangle = -|x_2\rangle \quad (A2)$$

which gives the corresponding T_{1u} irrep component

$$D_{ij}^{T_1}(r_1) = \langle x_2|Ir_1|x_1\rangle = -1 \quad (A3)$$

The octahedral group algebra can be simplified by considering carefully the subgroups of O . In addition, there are more idempotent splittings and wave solutions associated with octahedral symmetry. Moreover, D_4 and T are subgroups of O . Splitting with idempotents leaves two subchoices. One is free to use $D_4 \supset C_4$. Both tetragonal and trigonal base D matrices are present as derive in ref. [3].

Appendix A.5. T₂-Mode Trigonal Base D-Matrix

$$\begin{aligned}
 1 &= \begin{bmatrix} 1 & \cdot & \cdot \\ \cdot & 1 & \cdot \\ \cdot & \cdot & 1 \end{bmatrix}, R_1^2 = \begin{bmatrix} -\frac{1}{3} & -\frac{\sqrt{2}}{3} & \frac{\sqrt{6}}{3} \\ \cdot & -\frac{2}{3} & -\frac{\sqrt{3}}{3} \\ \frac{\sqrt{6}}{3} & -\frac{\sqrt{3}}{3} & \cdot \end{bmatrix}, R_2^2 = \begin{bmatrix} -\frac{1}{3} & -\frac{\sqrt{2}}{3} & -\frac{\sqrt{6}}{3} \\ -\frac{\sqrt{2}}{3} & -\frac{2}{3} & \frac{\sqrt{3}}{3} \\ -\frac{\sqrt{6}}{3} & \frac{\sqrt{3}}{3} & \cdot \end{bmatrix}, R_3^2 = \begin{bmatrix} -\frac{1}{3} & \frac{\sqrt{8}}{3} & \cdot \\ \frac{\sqrt{8}}{3} & \frac{1}{3} & \cdot \\ \cdot & \cdot & 1 \end{bmatrix} \\
 i_4 &= \begin{bmatrix} 1 & \cdot & \cdot \\ \cdot & 1 & \cdot \\ \cdot & \cdot & -1 \end{bmatrix}, R_3 = \begin{bmatrix} -\frac{1}{3} & -\frac{\sqrt{2}}{3} & -\frac{\sqrt{6}}{3} \\ -\frac{\sqrt{2}}{3} & -\frac{2}{3} & \frac{\sqrt{3}}{3} \\ \frac{\sqrt{6}}{3} & -\frac{\sqrt{3}}{3} & \cdot \end{bmatrix}, R_3^3 = \begin{bmatrix} -\frac{1}{3} & -\frac{\sqrt{2}}{3} & \frac{\sqrt{6}}{3} \\ -\frac{\sqrt{2}}{3} & -\frac{2}{3} & \frac{\sqrt{3}}{3} \\ -\frac{\sqrt{6}}{3} & \frac{\sqrt{3}}{3} & \cdot \end{bmatrix}, i_3 = \begin{bmatrix} -\frac{1}{3} & \frac{\sqrt{8}}{3} & \cdot \\ \frac{\sqrt{8}}{3} & \frac{1}{3} & \cdot \\ \cdot & \cdot & -1 \end{bmatrix} \\
 r_1 &= \begin{bmatrix} 1 & \cdot & \cdot \\ \cdot & -\frac{1}{2} & -\frac{\sqrt{3}}{2} \\ \cdot & \frac{\sqrt{3}}{2} & -\frac{1}{2} \end{bmatrix}, r_2 = \begin{bmatrix} -\frac{1}{3} & -\frac{\sqrt{2}}{3} & \frac{\sqrt{6}}{3} \\ -\frac{\sqrt{2}}{3} & -\frac{2}{3} & \frac{\sqrt{3}}{3} \\ -\frac{\sqrt{6}}{3} & \frac{\sqrt{3}}{3} & \cdot \end{bmatrix}, r_3 = \begin{bmatrix} -\frac{1}{3} & -\frac{\sqrt{2}}{3} & -\frac{\sqrt{6}}{3} \\ \cdot & -\frac{1}{6} & -\frac{\sqrt{3}}{6} \\ \cdot & -\frac{\sqrt{3}}{2} & \frac{1}{2} \end{bmatrix}, r_4 = \begin{bmatrix} -\frac{1}{3} & \frac{\sqrt{8}}{3} & \cdot \\ \frac{\sqrt{8}}{3} & -\frac{1}{6} & \frac{\sqrt{3}}{6} \\ \cdot & \frac{\sqrt{3}}{6} & \frac{1}{2} \end{bmatrix} \\
 i_2 &= \begin{bmatrix} 1 & \cdot & \cdot \\ \cdot & -\frac{1}{2} & \frac{\sqrt{3}}{2} \\ \cdot & \frac{\sqrt{3}}{2} & \frac{1}{2} \end{bmatrix}, i_1 = \begin{bmatrix} -\frac{1}{3} & -\frac{\sqrt{2}}{3} & -\frac{\sqrt{6}}{3} \\ -\frac{\sqrt{2}}{3} & -\frac{2}{3} & \frac{\sqrt{3}}{3} \\ -\frac{\sqrt{6}}{3} & \frac{\sqrt{3}}{3} & \cdot \end{bmatrix}, R_2 = \begin{bmatrix} -\frac{1}{3} & -\frac{\sqrt{2}}{3} & \frac{\sqrt{6}}{3} \\ \frac{\sqrt{8}}{3} & -\frac{1}{6} & \frac{\sqrt{3}}{6} \\ \cdot & -\frac{\sqrt{3}}{2} & -\frac{1}{2} \end{bmatrix}, R_1 = \begin{bmatrix} -\frac{1}{3} & \frac{\sqrt{8}}{3} & \cdot \\ -\frac{\sqrt{2}}{3} & -\frac{1}{6} & \frac{\sqrt{3}}{6} \\ -\frac{\sqrt{6}}{3} & -\frac{\sqrt{3}}{6} & -\frac{1}{2} \end{bmatrix} \\
 r_1^2 &= \begin{bmatrix} 1 & \cdot & \cdot \\ \cdot & \frac{1}{2} & -\frac{\sqrt{3}}{2} \\ \cdot & -\frac{\sqrt{3}}{2} & -\frac{1}{2} \end{bmatrix}, r_2^2 = \begin{bmatrix} -\frac{1}{3} & -\frac{\sqrt{2}}{3} & -\frac{\sqrt{6}}{3} \\ -\frac{\sqrt{2}}{3} & -\frac{2}{3} & \frac{\sqrt{3}}{3} \\ \frac{\sqrt{6}}{3} & \frac{\sqrt{3}}{3} & \cdot \end{bmatrix}, r_3^2 = \begin{bmatrix} -\frac{1}{3} & \frac{\sqrt{8}}{3} & \cdot \\ -\frac{\sqrt{2}}{3} & -\frac{1}{6} & -\frac{\sqrt{3}}{6} \\ -\frac{\sqrt{6}}{3} & -\frac{\sqrt{3}}{6} & \frac{1}{2} \end{bmatrix}, r_4^2 = \begin{bmatrix} -\frac{1}{3} & -\frac{\sqrt{2}}{3} & \frac{\sqrt{6}}{3} \\ \frac{\sqrt{8}}{3} & -\frac{1}{6} & \frac{\sqrt{3}}{6} \\ \cdot & \frac{\sqrt{3}}{6} & \frac{1}{2} \end{bmatrix} \\
 i_5 &= \begin{bmatrix} 1 & \cdot & \cdot \\ \cdot & -\frac{1}{2} & -\frac{\sqrt{3}}{2} \\ \cdot & \frac{\sqrt{3}}{2} & -\frac{1}{2} \end{bmatrix}, i_6 = \begin{bmatrix} -\frac{1}{3} & -\frac{\sqrt{2}}{3} & -\frac{\sqrt{6}}{3} \\ -\frac{\sqrt{2}}{3} & -\frac{2}{3} & \frac{\sqrt{3}}{3} \\ \frac{\sqrt{6}}{3} & \frac{\sqrt{3}}{3} & \cdot \end{bmatrix}, R_2^3 = \begin{bmatrix} -\frac{1}{3} & \frac{\sqrt{8}}{3} & \cdot \\ -\frac{\sqrt{2}}{3} & -\frac{1}{6} & -\frac{\sqrt{3}}{6} \\ \frac{\sqrt{6}}{3} & \frac{\sqrt{3}}{6} & -\frac{1}{2} \end{bmatrix}, R_1^3 = \begin{bmatrix} -\frac{1}{3} & \cdot & -\frac{\sqrt{6}}{3} \\ \cdot & -\frac{1}{6} & \frac{\sqrt{3}}{6} \\ \cdot & \frac{\sqrt{3}}{2} & -\frac{1}{2} \end{bmatrix}
 \end{aligned}$$

Appendix A.6. E-Mode Trigonal Bases D-Matrix

$$\begin{aligned}
 1 &= \begin{bmatrix} 1 & \cdot \\ \cdot & 1 \end{bmatrix}, R_1^2 = \begin{bmatrix} 1 & \cdot \\ \cdot & 1 \end{bmatrix}, R_2^2 = \begin{bmatrix} 1 & \cdot \\ \cdot & 1 \end{bmatrix}, R_3^2 = \begin{bmatrix} 1 & \cdot \\ \cdot & 1 \end{bmatrix} \\
 i_4 &= \begin{bmatrix} 1 & \cdot \\ \cdot & -1 \end{bmatrix}, R_3 = \begin{bmatrix} 1 & \cdot \\ \cdot & -1 \end{bmatrix}, R_3^3 = \begin{bmatrix} 1 & \cdot \\ \cdot & -1 \end{bmatrix}, i_3 = \begin{bmatrix} 1 & \cdot \\ \cdot & -1 \end{bmatrix} \\
 r_1 &= \begin{bmatrix} -\frac{1}{2} & -\frac{\sqrt{3}}{2} \\ \frac{\sqrt{3}}{2} & -\frac{1}{2} \end{bmatrix}, r_2 = \begin{bmatrix} -\frac{1}{2} & -\frac{\sqrt{3}}{2} \\ \frac{\sqrt{3}}{2} & -\frac{1}{2} \end{bmatrix}, r_3 = \begin{bmatrix} -\frac{1}{2} & -\frac{\sqrt{3}}{2} \\ \frac{\sqrt{3}}{2} & -\frac{1}{2} \end{bmatrix}, r_4 = \begin{bmatrix} -\frac{1}{2} & -\frac{\sqrt{3}}{2} \\ \frac{\sqrt{3}}{2} & -\frac{1}{2} \end{bmatrix} \\
 i_5 &= \begin{bmatrix} -\frac{1}{2} & -\frac{\sqrt{3}}{2} \\ \frac{\sqrt{3}}{2} & \frac{1}{2} \end{bmatrix}, R_2 = \begin{bmatrix} -\frac{1}{2} & \frac{\sqrt{3}}{2} \\ \frac{\sqrt{3}}{2} & \frac{1}{2} \end{bmatrix} \\
 i_1 &= \begin{bmatrix} -\frac{1}{2} & \frac{\sqrt{3}}{2} \\ \frac{\sqrt{3}}{2} & \frac{1}{2} \end{bmatrix}, i_2 = \begin{bmatrix} -\frac{1}{2} & \frac{\sqrt{3}}{2} \\ \frac{\sqrt{3}}{2} & \frac{1}{2} \end{bmatrix}, R_2 = \begin{bmatrix} -\frac{1}{2} & \frac{\sqrt{3}}{2} \\ \frac{\sqrt{3}}{2} & \frac{1}{2} \end{bmatrix}, R_1 = \begin{bmatrix} -\frac{1}{2} & \frac{\sqrt{3}}{2} \\ \frac{\sqrt{3}}{2} & \frac{1}{2} \end{bmatrix} \\
 r_1^2 &= \begin{bmatrix} -\frac{1}{2} & \frac{\sqrt{3}}{2} \\ -\frac{\sqrt{3}}{2} & -\frac{1}{2} \end{bmatrix}, r_2^2 = \begin{bmatrix} -\frac{1}{2} & -\frac{\sqrt{3}}{2} \\ \frac{\sqrt{3}}{2} & -\frac{1}{2} \end{bmatrix}, r_3^2 = \begin{bmatrix} -\frac{1}{2} & -\frac{\sqrt{3}}{2} \\ \frac{\sqrt{3}}{2} & -\frac{1}{2} \end{bmatrix}, r_4^2 = \begin{bmatrix} -\frac{1}{2} & -\frac{\sqrt{3}}{2} \\ \frac{\sqrt{3}}{2} & -\frac{1}{2} \end{bmatrix} \\
 i_5 &= \begin{bmatrix} -\frac{1}{2} & -\frac{\sqrt{3}}{2} \\ \frac{\sqrt{3}}{2} & \frac{1}{2} \end{bmatrix}, i_6 = \begin{bmatrix} -\frac{1}{2} & \frac{\sqrt{3}}{2} \\ \frac{\sqrt{3}}{2} & \frac{1}{2} \end{bmatrix}, R_2^3 = \begin{bmatrix} -\frac{1}{2} & \frac{\sqrt{3}}{2} \\ \frac{\sqrt{3}}{2} & \frac{1}{2} \end{bmatrix}, R_1^3 = \begin{bmatrix} -\frac{1}{2} & \frac{\sqrt{3}}{2} \\ \frac{\sqrt{3}}{2} & \frac{1}{2} \end{bmatrix}
 \end{aligned}$$

References

1. Papoušek, D.; Aliev, M.R. *Molecular Vibrational and Rotational Spectra*. In *Studies in Physical and Theoretical Chemistry*; Elsevier Scientific Publishing Company: Amsterdam, The Netherlands; Oxford, UK; New York, NY, USA, 1982; Volume 17, pp. 195–324.
2. Herzberg, G. *Infrared and Raman Spectra of Polyatomic Molecules*; Van Nostrand Reinhold LTD: New York, NY, USA, 1945.
3. Harter, W.G. *Principle of Symmetry, Dynamics & Spectroscopy*; Wiley: New York, NY, USA, 1993.
4. Bunker, P.R.; Jensen, P. *Molecular Symmetry and Spectroscopy*, 2nd ed.; NRC Research Press: Ottawa, ON, Canada, 1998.
5. Crogman, H.T.; Harter, W.G. Frame transformation relations for fluxional symmetric rotor dimmers. *J. Chem. Phys.* **2004**, *121*, 9297–9312. [[CrossRef](#)] [[PubMed](#)]

6. Crogman, H.T. A rotational energy surface study for low polyad structures of the general rovibrational Hamiltonian. *Mol. Phys.* **2010**, *108*, 705–772. [[CrossRef](#)]
7. Chen, J.Q. *Group Representation Theory for Physicist*; World Scientific Publishing Co. Pte. Ltd.: Singapore, 1989.
8. Harter, W.G. *The Quantum Computer Age*; University of Arkansas: Fayetteville, AR, USA, 2004.
9. Álvarez-Bajo, O.; Lemus, R.; Carvajal, M.; Pérez-Bernal, F. Symmetry projection of the rovibrational functions of methane. *AIP Conf. Proc. Am. Inst. Phys.* **2010**, *1323*, 191–202.
10. Alvarez-Bajo, O.; Lemus, R.; Carvajal, M.; Perez-Bernal, F. Equivalent rotations associated with the permutation inversion group revisited: Symmetry projection of the rotational functions of methane. *Mol. Phys.* **2011**, *109*, 797–812. [[CrossRef](#)]
11. Crogman, H.T.; Choi, B.; Chen, H.B.; Harter, W.G. Frame Transformation Relations and Symmetry Analysis of Fluxional Symmetric Rotor Dimers. *Symmetry* **2013**, *5*, 86–118. [[CrossRef](#)]
12. Harter, W. Theory of hyperfine and super levels in symmetric polyatomic molecules. II Elementary cases in octahedral hexafluoride molecules. *Phys. Rev. A* **1981**, *24*, 192–263. [[CrossRef](#)]
13. Harter, W.G.; Patterson, C.W.; da Paixao, F.J. Frame transformation relations and multiple transitions in symmetric polyatomic molecules. *Rev. Mod. Phys.* **1978**, *50*, 37–83. [[CrossRef](#)]
14. Harter, W.G.; Patterson, C.W. Rotational energy surfaces and high-J eigenvalue structure of polyatomic molecules. *J. Chem. Phys.* **1984**, *80*, 4241–4261. [[CrossRef](#)]
15. Harter, W.; Patterson, C.W. Theory of hyperfine and super levels in symmetric polyatomic molecules. Trigonal and tetrahedral: Elementary spin $\frac{1}{2}$ cases vibronic ground states. *Phys. Rev. A* **1979**, *19*, 2277–2303. [[CrossRef](#)]
16. Harter, W.G. Alternative basis for the theory of complex spectra. *Phys. Rev. A* **1973**, *8*, 2819–2827. [[CrossRef](#)]
17. Harter, W.G.; Patterson, C.W. Alternative basis for the theory of complex spectra II. *Phys. Rev. A* **1976**, *13*, 1067–1082. [[CrossRef](#)]
18. Patterson, C.W.; Harter, W.G. Canonical symmetrization for unitary bases. I. Canonical Weyl bases. *J. Math. Phys.* **1976**, *17*, 1125–1136. [[CrossRef](#)]
19. Boudon, V. Habilitation à Diriger des Recherches. Doctoral Dissertation, Université de Bourgogne, Dijon, France, 2004.
20. Wenger, C.h.; Champion, J.P. Spherical top data system (STDS) software for the simulation of spherical top spectra. *J. Quant. Spectrosc. Radiat. Transf.* **1998**, *59*, 471–480. [[CrossRef](#)]
21. Wormer, P.E.S. Tetrahedral harmonics revisited. *Mol. Phys.* **2001**, *99*, 1973–1980. [[CrossRef](#)]

Disclaimer/Publisher's Note: The statements, opinions and data contained in all publications are solely those of the individual author(s) and contributor(s) and not of MDPI and/or the editor(s). MDPI and/or the editor(s) disclaim responsibility for any injury to people or property resulting from any ideas, methods, instructions or products referred to in the content.